Interactions of Pigeon Guillemots and Rhinoceros Auklets with the marine environment

Liam Pendleton

A thesis

submitted in partial fulfillment of the

requirements for the degree of

Master of Science

University of Washington

2019

Committee:

Sarah J. Converse, Chair

Mark Scheuerell

Eric Wagner

Program Authorized to Offer Degree:

School of Aquatic and Fishery Sciences

University of Washington

Abstract

Interactions of Pigeon Guillemots and Rhinoceros Auklets with the marine environment

Liam Pendleton

Chair of the Supervisory Committee:

Sarah J. Converse

Unit Leader, USGS Washington Cooperative Fish and Wildlife Research Unit

Associate Professor, School of Environmental and Forest Sciences & School of Aquatic and Fishery Sciences, University of Washington

Pigeon Guillemots (*Cepphus columba*) and Rhinoceros Auklets (*Cerorhinca monocerata*) are seabirds with a widespread year-round distribution throughout the Salish Sea, where they have a long history of study. They have been identified as Puget Sound Vital Signs, i.e., indicators, by the Puget Sound Partnership. The purpose of a Vital Sign is to act as a benchmark measure of the ecological health of Puget Sound and to guide recovery goals. Despite their status as indicators, major gaps exist in our knowledge of their relationship to the marine environment, including the relationship between marine conditions and their demography, and characteristics of their foraging habitat. These knowledge gaps limit their utility as indicators. In this thesis, I address some of these gaps using data from Protection Island in the Salish Sea.

In Chapter 1, I developed hierarchical models in a Bayesian framework to understand the relationships between Pigeon Guillemot reproductive outcomes and oceanographic conditions. I considered the influence of multiple indicators of oceanographic conditions across different temporal scales relative to the breeding season to learn how the temporal occurrence of these conditions influences Pigeon Guillemot breeding outcomes. Pigeon Guillemot reproductive success, defined as the probability of a nest fledging at least one chick, was positively correlated with the North Pacific Gyre Oscillation (NPGO) index. Higher NGPO values are indicators of increased upwelling in the northeast Pacific and higher marine productivity. Guillemot reproductive success did not appear to be related to local marine conditions, including sea surface temperature or chlorophyll-a concentration, or by the broader conditions described by the Pacific Decadal Oscillation. The lack of influence of any other covariate that I considered may be explained by the Pigeon Guillemots' generalist nature, in particular their ability to prey switch depending on the abundance or quality of prey species available to them, which may buffer them against variability in marine conditions. My results provide a better understanding of how the Pigeon Guillemot population at Protection Island responds to marine conditions and informs their use as a Puget Sound indicator species.

In Chapter 2, I conducted preliminary analyses of the behavior-specific movements of Pigeon Guillemots and Rhinoceros Auklets nesting at Protection Island. I tracked individuals during the breeding seasons of 2022 and 2023 and used these location data to fit discrete-time hidden Markov models to characterize behavioral states of both species, which have very different foraging and provisioning strategies during the breeding season. I used step length and turn angle to model movements of tracked birds across resting, transiting, and foraging states. Fitted models largely conflated movements associated with resting and foraging states, and predicted that foraging behavior occurred on or near Protection Island. These findings suggest the importance of fixing the resting state in these models, given that we know when and where resting, or stationary, behavior is primarily occurring, such that the models are only distinguishing transit and foraging states. I discuss future directions for this analysis.

The utility of Pigeon Guillemots and Rhinoceros Auklets as indicators of environmental conditions in the Salish Sea is contingent on our understanding of how they respond to and use their habitat. Together, these chapters explore aspects of their breeding ecology and behavior and suggest processes through which we can productively view their relationship with the environment in the Salish Sea.

TABLE OF CONTENTS

LIST OF FIGURES

LIST OF TABLES

ACKNOWLEDGEMENTS

I would first like to thank my funding sources, including the School of Aquatic and Fishery Sciences at the University of Washington; the Washington Cooperative Fish and Wildlife Research Unit; the US Fish and Wildlife Service; the Wilson Ornithological Society; and the SeaDoc Society through the Karen C. Drayer Wildlife Health Center, School of Veterinary Medicine, University of California, Davis. I would like to acknowledge and express gratitude to Scott Pearson, Peter Hodum, Sue Thomas, Eric Wagner, Chad Norris, and all other collaborators who played a role in facilitating the field work that went into this thesis. I would like to acknowledge Lee Robinson and her daughter Karen Robinson, whose efforts in monitoring Pigeon Guillemot nests at Protection Island for 18 years made the first chapter of this thesis possible. I would like to thank my cohort and community at SAFS for providing me with a sense of belonging and companionship. Many thanks to the Quantitative Conservation Lab members and Sarah Romero, who made my life and my work easier and more enjoyable, and who supported me through these past three years. I would like to express gratitude to my committee, Mark Scheuerell and Eric Wagner, who provided me with great support and guidance, feedback on this thesis, and whose efforts supported this project and saw it through to completion. Finally, I would like to express my deepest gratitude to my advisor, Sarah J. Converse. Thank you for providing me with the opportunity to work with you, to learn from and with you, for your mentorship, support, and for your unending patience. Your example has facilitated my growth as both a scientist and an individual.

Chapter 1: Estimating the influence of environmental conditions on breeding outcomes in Pigeon Guillemots (*Cepphus columba*)

Publication history: This study was co-authored with L Robinson, EL Wagner, SF Pearson, SM Thomas, and SJ Converse. At the time this thesis was published, this chapter was not in review with a journal.

1.1 ABSTRACT

Seabirds are useful indicators of the marine environment due to their conspicuous nature, widespread distribution, and long history of study. The Pigeon Guillemot has been identified as an indicator of conditions in Puget Sound, Washington, USA, and has been monitored in the region for the past few decades, yet little is known about how they respond to marine conditions in the Salish Sea. In this study, we investigated the influence of marine conditions on breeding outcomes of Pigeon Guillemots at Protection Island National Wildlife Refuge, Washington. We used nest boxes to monitor nest development for two years, adding onto an 18-year historic dataset from the island. We developed a model to predict breeding outcomes, defined as nest success (the probability that a nest produces at least one fledgling) and double fledging (the probability that a nest produces two fledglings, given that it produces at least one), as a function of both local and spatially-broad marine conditions. We explored the effects of sea surface temperature, chlorophyll-a concentration, and marine conditions described by the North Pacific Gyre Oscillation and Pacific Decadal Oscillation indices across five temporal windows. We found a positive correlation between nesting success and the NPGO index, but we found no evidence of a relationship between other oceanic processes and breeding outcomes. Our findings suggest that guillemots at Protection Island may be relatively robust in their ability to adjust to less productive conditions, which may be attributed to their generalist diets. Our findings illustrate this population's flexibility in accommodating adverse conditions and better inform the use of this species as an indicator of conditions in Puget Sound.

1.2 INTRODUCTION

Oceanographic conditions have direct effects on the distribution, quality, and quantity of food available to seabirds (McGowan et al., 1998; Barbar and Chavez, 2002; Cury et al., 2011), and thereby have indirect effects on habitat use and demography. Oceanographic processes that cause low-nutrient conditions leading to decreased prey abundance can result in lower body condition, decreased chick provisioning rates, and nest failure, ultimately reducing reproductive success and, potentially, abundance (McGowan et al., 1998; Barber and Chavez, 2002; Sandvik et al., 2012). Due to their reliance on the marine environment, their global distribution, and the existence of long-term monitoring datasets, seabirds have been identified as indicators of marine conditions (Piatt et al., 2007; Parsons et al., 2008; Mallory et al., 2010). Furthermore, they are among the most threatened groups of birds worldwide (Croxall et al., 2012), highlighting the need to better understand how habitat changes in the oceans, which are likely to accelerate in a changing climate, may affect their populations (Grémillet and Boulinier, 2009).

Local oceanographic processes have documented relationships with habitat use and demography in seabirds. Sea surface temperature is frequently used as an indicator of marine productivity (Hayward, 1997). For instance, lower sea surface temperatures positively affect plankton growth and fish movement, which in turn positively impacts Black-legged Kittiwake (*Rissa tridactyla*) feeding conditions and productivity (Carroll et al., 2015). Sea surface temperature is also negatively correlated with breeding propensity in Cassin's Auklets (*Ptychoramphus aleuticus*) (Lee et al., 2007), and survival in Brandt's Cormorants (*Phalacrocorax penicillatus*) (Schmidt et al., 2015). Frederiksen et al. (2007) report a negative relationship between winter sea surface temperature and Black-legged Kittiwake productivity, suggesting lagged, or carry-over, effects of marine conditions. Upwelling processes in the northeast Pacific transport cold, nutrient-rich water to the surface, which increases chlorophyll-a concentration and results in indirect impacts on organisms at higher trophic levels (McGowan et al., 1998; Arnott and Ruxton, 2002; Mallory et al., 2007). This chlorophyll-a concentration is commonly used as a proxy for primary productivity through its indication of phytoplankton abundance (Huot et al., 2007).

Phytoplankton abundance has a bottom-up influence on species at higher trophic levels, such as seabirds, that rely on the forage fish that feed on phytoplankton (Pinaud and Weimerkirch, 2006). For instance, Rhinoceros Auklets (*Cerorhinca monocerata*) experienced reduced chick growth and altered breeding phenology following prolonged marine warming and subsequent reduction of chlorophyll-a concentration during the 1997-1998 El Niño in Washington State, USA (Wilson, 2005). Consequently, chlorophyll-a concentration is commonly used to identify breeding seabird foraging habitat and to assess bottom-up effects on their productivity (Grémillet et al., 2008; Thompson et al., 2012).

Spatially broad indices of oceanographic conditions are also predictors of seabird demography, as the conditions associated with these indices shape prey assemblages and distributions. The Pacific Decadal Oscillation (PDO) is a physical phenomenon of climatic variability across the north Pacific. The PDO consists of warm and cool phases, oscillating on the scale of 20 – 30 years between higher pressure, warmer waters along the Pacific coast (positive index values) and lower pressure, cooler waters on the Pacific coast (negative index values) (Zhang et al., 1997; Mantua and Hare, 2002). Seabird abundance in Hawaii and California is negatively correlated with the PDO index, indicating that seabird populations benefit during cooler phases associated with greater marine productivity (Vandenbosch, 2000). Additionally, warm phases of the PDO correlate with lower nutrient density and increased dietary stress in Rhinoceros Auklets (*Cerorhinca monocerata*), suggesting the potential for a resulting decrease in reproductive success (Shimabukuro et al., 2023). The North Pacific Gyre Oscillation (NPGO) is a climate pattern in the northeast Pacific that indexes fluctuations in key features of the marine system, including salinity, chlorophyll-a concentration, and other nutrients within the California Current system and the Gulf of Alaska (Di Lorenzo et al., 2008). The NPGO index describes alternating periods of high and low pressure over the North Pacific and likewise consists of positive phases, describing stronger upwelling and increased productivity, and negative phases, which describe weaker upwelling and decreased productivity. These phases play roles in driving changes in seabird demography. For example, Northern Fulmar (*Fulmarus glacialis*) abundance has been linked with oceanic conditions described by positive

NPGO phases two months prior to their presence in a foraging area, indicating lagged effects of the ocean conditions described by the NPGO (Studwell et al., 2017).

An understanding of the relationships between seabirds and marine conditions is important to interpret the environmental signals that seabirds provide regarding the health of marine ecosystems. Pigeon Guillemots (*Cepphus columba;* hereafter, guillemots) have been identified as ecosystem indicators in Puget Sound, Washington, USA due to their strong dependence on the marine ecosystem, the availability of long-term datasets, and the existence of ongoing monitoring programs (Pearson and Hamel, 2013). While diet and breeding phenology of this species have been studied in Puget Sound (Bishop et al., 2014; Buckner et al., 2022; Warlick, 2022), there has been little effort to understand how marine conditions influence guillemot populations.

We modeled breeding outcomes of guillemots at Protection Island, Washington as a function of covariates describing marine conditions at a range of temporal scales. We fit the models to long-term data on guillemot breeding outcomes in nest boxes at Protection Island, including data from 1996 – 2013 and 2022 – 2023. We evaluated evidence for several hypotheses. We hypothesized a positive relationship between chlorophyll-a concentration and guillemot breeding success due to the positive relationship between chlorophyll-a and forage fish abundance. Next, we hypothesized a positive relationship between breeding success and the North Pacific Gyre Oscillation index due to the increased nutrients linked with positive values of the index. We hypothesized a negative relationship between sea surface temperature and guillemot breeding success because of the increased nutrients associated with cooler waters. Finally, we hypothesized a negative relationship between the Pacific Decadal Oscillation index and guillemot breeding success due to the greater marine productivity associated with negative values of the PDO. Finally, we hypothesized that these oceanographic phenomena would be most influential on guillemot breeding success prior to the onset of the breeding season, due to the time required for bottom-up effects to propagate through the food web.

1.3 METHODS

1.3.1 Study Species & System

Guillemots are members of the auk family (*Alcidae*). They are one of the few auk species that lays 1- to 2-egg clutches, rather than exclusively 1-egg clutches (Emms and Verbeek, 1991; Santo and Nelson, 1995). They are nearshore foragers and dive in shallow waters to feed on demersal species (Litzow et al., 2004; Johns and Warzybok, 2022). They typically feed on gunnel (*Pholis* spp.), sculpin (*Leptocottus* spp.) and rockfish (*Sebastes* spp.), although they have also been observed foraging for higher-lipid schooling fishes, including Pacific sand lance (*Ammodytes hexapterus*) and Pacific herring (*Clupea pallasii*) (Golet et al., 2000; Litzow and Piatt, 2003; Buckner et al., 2022).

This study took place at Protection Island (48°07'38.2"N, 122°55'45.5"W) in Washington, USA, in the Strait of Juan de Fuca. The island has a land area of 153 hectares and is closed to the public. The island is owned primarily by the US Fish and Wildlife Service and is designated as Protection Island National Wildlife Refuge, though one portion of the island is owned by Washington Department of Fish and Wildlife and is designated as the Zella M. Schultz Seabird Sanctuary. Protection Island hosts a breeding population of guillemots previously estimated at 1,200 individuals (S. Thomas, USFWS, 2023, unpublished data). It includes seabird breeding habitat in the form of steep cliff faces and bluffs, as well as driftwood-covered beaches. In addition to guillemots, Tufted Puffins (*Fratercula cirrhata*), Rhinoceros Auklets (*Cerorhinca monocerata*), Olympic Gulls (*Larus glaucescens* x *occidentalis*), Pelagic Cormorants (*Phalacrocorax pelagicus*), and other seabirds breed on Protection Island. No mammalian nest predators are found on Protection Island, other than river otters (*Lontra canadensis*).

1.3.2 Data

1.3.2.1 Nest Box Monitoring and Breeding Outcomes

We used wooden nest boxes to monitor guillemots. In 1996 – 2013, nest boxes were located in the marina and the area just to the southwest of the marina. In 2022, nest boxes were located along the southern shore of the island to the marina (Figure 1.1). In 2023, nest boxes were located in similar areas

to 2022 except that we also placed boxes on Violet Point to the north of the marina along the north shore (Figure 1.2). We fitted boxes with secure, removable lids allowing access to box contents and we weighted lids with rocks or driftwood to exclude nest predators. Boxes were set amongst driftwood along the shore in the early spring of each year prior to initiation of nesting, except for 13 boxes in the marina, which were partially buried and permanent.

We visited boxes weekly beginning in late May to track nest status over the course of the breeding season until approximately mid-September, when nesting activity ceased. At each visit, the contents of nest boxes were recorded, including the number of eggs, chicks, and adults. We captured chicks and adults by hand when we encountered them in nest boxes. All adults and any chicks that were large enough to band (≥150 g) received a uniquely numbered metal USGS band and three unique color bands. Bands were replaced if they showed excessive wear.

We recorded a new nest when we found eggs in a nest box. We summarized breeding outcomes using a categorical distribution with three potential outcomes. Nests could fail and produce no fledglings, they could produce one fledgling, or they could produce two fledglings. Because fledging is not directly observable, we assumed that chicks fledged successfully if they were absent from a nest at the first visit when they were certain to be old enough to have fledged (≥29 days; Ewins, 2020). This assumption implies that chicks that are old enough to fledge but that die in the nest box will be found in the nest box (i.e., will not be ejected by an adult nor removed by a scavenger). Given that our nest checks occurred weekly, we believe this to be a reasonable assumption. In total, we monitored 620 nests. There were five instances in the 1996 – 2013 data where chicks were recorded with no preceding egg presence, indicating a potential data entry error, so we removed these nests from the analysis. There were ten instances in which chicks were present through the final observation of a nest. Because nest fates were inconclusive, these records were censored and not included in the analysis. From the remaining 605 nests, we concluded that 473 chicks fledged in total, for an average of 0.78 chicks per nest (Table 1.1).

1.3.2.2 *Oceanographic Covariates*

We evaluated four potential predictors of nesting outcomes. The first two are local measures of marine conditions: sea surface temperature (SST) and chlorophyll-a concentration (CHLa). The second two describe broader marine conditions in the north Pacific Ocean: the Pacific Decadal Oscillation (PDO) and the North Pacific Gyre Oscillation (NPGO) indices. For all covariates, we obtained available data from 1995 through 2023. All covariate data were reported monthly, so we averaged these at five alternative temporal windows for each year, allowing us to explore the timing at which marine conditions may influence nesting outcomes of guillemots at Protection Island. These scales included (1) YearEarly, for monthly values averaged over May of year *t*-1 through April of year *t* (we symbolize this for a given covariate as, e.g., SST.YearEarly); (2) YearLate, for monthly values averaged over October of year *t*-1 through September of year *t,* e.g., SST.YearLate; (3) Winter, for monthly values averaged over October of year *t*-1 through March of year *t,* e.g., SST.Winter; (4) LateWinter, for monthly values averaged over January of year *t* through April of year *t,* e.g., SST.LateWinter; and (5) Breed, for monthly values averaged over May of year *t* through September of year *t,* e.g., SST.Breed.

We obtained monthly SST data from Race Rocks Lighthouse (Lu, 2023) located on the southern tip of Vancouver Island, British Columbia, Canada. These data had the fewest missing records of all available sources within the Strait of Juan de Fuca and nearby Admiralty Inlet. There were several missing values in the time series (~1%), and we used a random walk model embedded within the breeding outcomes analysis to estimate the missing values (see below).

We obtained monthly CHLa index values from the NOAA Unified Access Framework ERDDAP server. We specified the spatial extent of the region around Protection Island as falling between 48.360074°N – 47.993307°N and -123.306315°E – -122.694708°E, which encompasses the entirety of Sequim Bay, Discovery Bay, Port Townsend Bay, Admiralty Inlet, and a large part of the Strait of Juan de Fuca to the north of Protection Island. Two datasets were combined to cover the required years. The first of these was a dataset of monthly observations from 1997 – 2010 (NASA/GSFC OBPG, 2018), and the second was a dataset of monthly measures spanning 2011 – 2023 (NASA/GSFC OBPG, 2022).

Again, there were several missing values in the time series (~12%), and we used a random walk model embedded within the breeding outcomes analysis to estimate the missing values (see below).

Finally, we obtained monthly NPGO data from the NOAA/ESRL PSL webpage http://www.o3d.org/npgo/npgo.php (Di Lorenzo et al., 2008) and monthly PDO data from the NOAA National Centers for Environmental Information (Mantua, 1999). Both of these time series were complete.

1.3.3 Data Analysis

1.3.3.1 Modeling Missing Covariate Data

There were several missing values in the monthly SST (~1%) and CHLa (~12%) time series. To estimate these missing values, we used a simple random walk model:

$$log\ (X_{t=1}) \sim Normal(\mu_X, \sigma_X)$$

and, for t = 2:T:

$$log\ (X_t) \sim Normal(log(X_{t-1})\ , \sigma_X)$$

where $\boldsymbol{X}$ is the time series of values for either SST or CHLa, μ_Z is the estimated expectation of the first value in the time series, σ_Z is the estimated standard deviation of model errors, and T is the length of the time series, in months. Because the first value in the time series was not missing for SST, we omitted the equation for $log\ (X_{t=1})$, but we included it for CHLa, for which the first value was missing. We fit this model and then summarized the resulting complete time series based on our five temporal scales, described above.

1.3.3.2 Modeling Breeding Outcomes

We modeled the breeding outcome of nest i, y_i, as categorically distributed with probability vector ω_i:

$$y_i \sim \text{Categorical}\ (\omega_i)$$

and we modeled the probability vector as:

$$\omega_i = [1 - \phi_i \quad \phi_i(1 - \gamma_i) \quad \phi_i \gamma_i]$$

The parameter ϕ_i (which we refer to herein as "breeding success") is the probability that nest *i* produces at least one fledgling, while the parameter γ_i (which we refer to herein as "double fledging") is the probability that nest *i* produces two fledglings, conditional on it having produced at least one. Note that the probability vector ω_i (of length 3) sums to one.

We then modeled the parameters ϕ_i and γ_i as a function of environmental covariates relevant to the year *t* in which nest *i* occurred. We also included temporal random effects to account for residual temporal variation:

$$logit(\phi_i) = \boldsymbol{\beta}^{\phi} * \boldsymbol{X}_{t[i]} + \varepsilon^{\phi}_{t[i]}$$

and

$$logit(\gamma_i) = \boldsymbol{\beta}^{\gamma} * \boldsymbol{X}_{t[i]} + \varepsilon^{\gamma}_{t[i]}$$

where $\boldsymbol{\beta}^{\phi}$ is a vector of coefficients (of length equal to the number of covariates plus one for the intercept) for environmental covariates in the model for ϕ_i, $\boldsymbol{\beta}^{\gamma}$ is a vector of coefficients for environmental covariates in the model for γ_i, $\boldsymbol{X}_{t[i]}$ is a vector (with length equal to the relevant β) of environmental covariates in the year *t* in which nest *i* occurred (see *Oceanographic Covariates*, and note that $\boldsymbol{X}_{t[i]}$ need not be identical in the models of ϕ_i and γ_i), $\varepsilon^{\phi}_{t[i]}$ is the random effect of the year *t* in which nest *i* occurred in the model for ϕ_i, and $\varepsilon^{\gamma}_{t[i]}$ is the random effect of the year *t* in which nest *i* occurred in the model for γ_i. We modeled the random effects as:

$$\varepsilon^{\phi}_{t[i]} \sim Normal(0, \sigma^{\phi})$$

and

$$\varepsilon^{\gamma}_{t[i]} \sim Normal(0, \sigma^{\gamma}).$$

1.3.3.3 Priors and Model Implementation

We fit models using JAGS (Plummer, 2003) through R (R version 4.1.2). We fit the random walk and breeding outcome models in an integrated fashion, i.e., within the same Bayesian model (using a 2-stage model selection process, see below). We ran models for 50,000 iterations in three chains and

discarded the first 5,000 iterations as burn-in, and 135000 samples from the posterior. We assessed model convergence based on visual inspection of the trace plots and by assuring that the Gelman-Rubin statistic for all parameters was < 1.05. We specified priors as follows. For the models of missing covariates, we specified μ_X ~ Normal(0, 1) and σ_X ~ Uniform(0, 30). For the standard deviations of the random effects in the breeding outcomes models, we specified σ^{ϕ} and σ^{γ}~ Uniform(0,10). For the vector β^{Φ} and β^{γ} we specified intercepts as β_0^{Φ} and β_0^{γ} ~ Normal(0, 1). In the first stage of model selection, we also specified the priors for coefficients on the environmental covariates as $\beta_{1:K}^{\Phi}$ and $\beta_{1:K}^{\gamma}$ ~ Normal(0, 1) for *K* covariates. In the second stage of model selection, the priors on these coefficients were set dynamically (see *Model Selection*).

1.3.3.4 Model Selection

We undertook model selection in two steps. We first fit the nest model with each of the covariates at each of the five temporal scales one at a time for each parameter (ϕ and γ) individually, i.e., we fit 40 models, each with just one environmental covariate on either breeding success or double fledging, (we included the random effects of year in all models). For example, if we were fitting a model to evaluate the effect of, e.g., SST.Winter on ϕ, the model for γ would include no environmental covariate, just an intercept and the random effect of year. We calculated the Widely Applicable Information Criterion (WAIC; Watanabe, 2013) for each of these models. We then selected the temporal scale (i.e., YearEarly, YearLate, Winter, LateWinter, Breed) with the lowest WAIC value for each covariate (SST, CHLa, PDO, NPGO) for each parameter (ϕ, γ) and used this scale in the subsequent modeling.

In the second model selection step, we fit two models, each with the four covariates selected in the first step (one temporal scale for each of SST, CHLa, PDO, and NPGO for each of the two parameters) and we used the indicator variable approach, described by Kuo and Mallick (1998; see also Link and Barker, 2006; Converse et al., 2013), to select the combination of covariates that best predicted breeding success and double fledging. The model is written as:

$$logit(\phi_i) = \beta_0^{\phi} + \sum_{k=1}^{K} w_k * \beta_k^{\phi} * X_{t[i]} + \varepsilon_{t[i]}^{\phi}$$

and equivalently for γ_i, where w_k is the indicator variable for covariate *k*, with a prior of

$$w_k \sim Bernoulli(0.5).$$

Given four possible covariates on ϕ_i and four on γ_i, there are 2^8 possible models in the model set. Link and Barker (2006) noted that the priors on model parameters can influence the outcome of Bayesian model selection and recommended that the total prior variance of the linear predictor should remain constant regardless of the dimensions of the model when using the indicator variable approach for model selection. We therefore specified $\beta_{1:K[\phi]}^{\phi}$ and $\beta_{1:K[\gamma]}^{\gamma}$ ~ Normal(0, SD = $\left(\frac{K[\theta]}{V}\right)^{1/2}$) where $K[\theta]$ is the number of environmental covariates in the model for ϕ or γ (i.e., the number of covariates with w_k = 1), plus one for the intercept, at a particular model iteration. We then placed a Gamma-distributed prior on the precision of the linear predictor, *V*, with parameters 3.29 and 7.8, which produces a marginal distribution for the response variable that is approximately Uniform(0, 1) (Link and Barker, 2006).

We summarized the posterior samples to determine how often each of the candidate models was selected (based on the w_k) and treated the proportion of posterior samples in which a given model was sampled as a model weight (Kuo and Mallick, 1998; Link and Barker, 2006; Smith et al., 2011; Converse et al., 2013); we report all models with a model weight ≥ 1%. We also report the posterior inclusion probability, $w_{k|data}$, for each covariate, along with the Bayes Factor (BF) for each covariate, calculated as:

$$BF_k = \frac{w_{k|data}/(1 - w_{k|data})}{w_k/(1 - w_k)}.$$

Note that the denominator of the equation for Bayes Factor equals one (i.e., we placed equal prior odds on the inclusion of a parameter in the model). We report predicted breeding success and double fledging for the top two models (those that collectively make up nearly 50% total weight) and we report model-averaged estimates based on a weighted average of the estimates from these top two models.

1.4 RESULTS

1.4.1 Covariate Temporal Scales

The correlation was high (≥ 0.80) amongst the individual time scales for each covariate (Figure 1.3). There were quite small differences in the WAIC scores between these different temporal scales. Given the high covariance between the values across different temporal scales for a given covariate (ΔWAIC < 2.0), and because it was necessary for us to choose just one temporal scale for each before building further models, we chose the scale with the lowest WAIC score for each covariate. The best temporal scales for each covariate for breeding success (ϕ) were SST.Breed, CHLa.LateWinter, PDO.Breed, and NPGO.YearEarly (Table 1.2). Amongst these covariates, the largest correlation was 0.57 (between SST.Breed and PDO.Breed); the absolute value of all other correlations was < 0.5 (Figure 1.3). For double fledging (γ) the best temporal scales were SST.YearEarly, CHLa.Winter, PDO.Winter, and NPGO.LateWinter (Table 1.2). Amongst these covariates, the highest correlation was 0.74 (between SST.YearEarly and PDO.Winter); the absolute value of all other correlations was < 0.5 (Figure 1.3).

1.4.2 Breeding Outcomes

Only two models had weights > 10%, based on the second model selection step (Table 1.3). The highest-weighted model, with 32% model weight, included NPGO.YearEarly (during the year prior to breeding) as a predictor of breeding success (ϕ) and the null model for double fledging (γ). Again, we note that all models included the random effects, so "null" model in this context is the model without any environmental covariates. The second-best model included the null model for both breeding success and double fledging, with a weight of 14%. Every model that followed had a weight of less than 9% (Table 1.3).

The covariate with the highest posterior inclusion probability was NPGO.YearEarly in the model for breeding success (ϕ; Table 1.4), translating to BF = 2.14. All other covariates, across models for both breeding success and double fledging (γ) had a posterior inclusion probability ≤ 0.2, translating to BF ≤

0.25. Jeffreys (1961) proposed that a BF between 2 and 3 indicates weak support, while a BF between 3 and 12 indicates moderate support, and a BF > 12, strong support.

The posterior mean of breeding success (ϕ; Figure 1.4) and the posterior mean of double fledging (γ; Figure 1.5) from the top model were 0.58 (95% Credible Interval: 0.51 – 0.65) and 0.26 (0.21 – 0.31), respectively. There was a positive estimated effect of NPGO.YearEarly on ϕ, with a mean effect of 0.35 (0.11 – 0.61) from this model. From the second-highest performing (null) model, the estimates were 0.62 (0.54 – 0.69) for breeding success (Figure 1.4) and 0.26 (0.21 – 0.31) for double fledging. The model-averaged estimate of breeding success was 0.59 (0.52 – 0.67) and double fledging was 0.26 (0.21 – 0.31; Figure 1.5). There was a positive relationship between the NPGO index and breeding success (Figure 1.6).

1.5 DISCUSSION

We identified the NPGO index (in the year preceding the start of a given breeding season) as the only predictor of guillemot breeding success of the set of potential predictors that we considered. We estimated a positive relationship between NPGO.YearEarly and breeding success. However, there was only relatively weak evidence for this effect. Positive NPGO phases are associated with increased upwelling and greater plankton productivity through the spring and summer (Di Lorenzo et al., 2008; Chenillat et al., 2012). Guillemots typically provision chicks with gunnel and sculpin (Buckner et al., 2020), which primarily consume low-trophic organisms, including macrozooplankton that may respond readily to the effects of shifting NPGO values (De Forest and Busby, 2006; Tokranov, 2007). Cassin's Auklets (*Ptychoramphus aleuticus*) are zooplanktivorous seabirds (Burger and Powell, 1990) that are known to respond strongly to changes in NPGO due to its effects on their preferred prey. Schmidt et al. (2014) reported a strong positive relationship between NPGO and Cassin's Auklet reproductive success at Farallon National Wildlife Refuge, California, USA. They found the same relationship with Brandt's Cormorants (*Phalacrocorax penicillatus*), though for that species, reproductive success was influenced by NPGO in winter months. These links are consistent with Studwell et al. (2017), who reported a positive

association between Northern Fulmar (*Fulmarus glacialis*) abundance and NPGO. While the oceanic effects described by the NPGO appear to be drivers of seabird reproductive success in some systems, its effects on seabirds may vary latitudinally.

No other oceanographic covariates that we considered appeared to be related to guillemot breeding outcomes, suggesting that the population at Protection Island may be relatively robust to changing ocean conditions and may not be a sensitive indicator of marine conditions nor how these conditions influence other seabird species. Litzow et al. (2002) described breeding pairs of guillemots as being either specialists or generalists, with specialist pairs provisioning their chicks with higher-lipid fish such as Pacific sandlance (*Ammodytes hexapterus*) or Pacific herring (*Clupea pallasii*), increasing their reproductive success (Golet et al., 2000; Litzow et al., 2004). Guillemots are also known to prey-switch depending on the abundance of preferred prey species (Litzow et al., 2002). Guillemots on Whidbey Island, Washington, were observed to primarily forage on demersal species (Kuletz et al., 1983; Buckner et al., 2022), suggesting selection of a lower quality but more commonly available food source rather than one that is more variably abundant. There has been no organized study of guillemot food habits at Protection Island, though we have made anecdotal observations of adults delivering demersal species to nests.

The extended northeast Pacific marine heatwave of 2014 – 2015, colloquially known as "The Blob," resulted in anomalously warm surface water exceeding 2.5℃ above mean values. This event had widespread impacts on marine life, including the die-off of over 9,000 Cassin's Auklets due to a reduction in planktonic productivity (Jones et al., 2018), and reduced reproductive success of Rhinoceros Auklets at Protection Island (Wagner et al., 2023). The heatwave has been linked to a potential interaction between effects described by the NPGO and the PDO, resulting in prolonged warm marine temperatures, weak upwelling, and low productivity (Di Lorenzo and Mantua, 2016; Joh and Di Lorenzo, 2017). Given multiple climatological analyses over the past few decades that suggest shifting frequency of basin-scale oceanographic phenomena such as the El Niño Southern Oscillation (Timmerman et al., 1999; Cai et al., 2014), and warmer ambient sea surface temperature (Cane et al., 1997; Seager et al., 2019), further

exploration of how guillemots respond to short and long-term changes in the marine environment may provide a better understanding of the limits of their robustness to changing marine conditions.

Understanding the relationships between oceanographic conditions and seabird demography is vital for prediction and comprehension of seabirds' responses to environmental change. This study provides insights into the dynamics between oceanographic covariates and the breeding outcomes of guillemots at Protection Island. By illustrating the relationship between oceanic effects described by the NPGO and guillemot breeding outcomes, this research contributes to a growing body of literature on the drivers of seabird population dynamics. The model developed in this study provides a framework for assessing the impacts of various covariates on two important seabird demographic parameters. However, our findings also highlight gaps in our knowledge about guillemot ecology that may hinder our ability to interpret signals that they provide as a Puget Sound indicator species and suggest that guillemots may not be ideal indicators of how marine conditions impact seabird species. Future research may be focused on exploring some of these gaps, including the influence of other potential environmental predictors of reproductive success, or the influence of provisioning behavior of parents, such as provisioning rate or prey selection.

1.6 REFERENCES

Arnott, S. A., & Ruxton, G. D. (2002). Sandeel recruitment in the North Sea: demographic, climatic and trophic effects. Marine Ecology Progress Series, 238, 199–210. https://doi.org/10.3354/meps238199

Barber, R. T., & Chavez, F. P. (1983). Biological consequences of El Niño. Science, 222(4629), 1203–1210. https://doi.org/10.1126/science.222.4629.1203

Bishop, E., Rosling, G., Kind, P., & Wood, F. (2016). Pigeon Guillemots on Whidbey Island, Washington: a six-year monitoring study. *Northwestern Naturalist*, *97*(3), 237–245. https://doi.org/10.1898/NWN15-31.1

Buckner, E., Chittaro, P., Wood, F., & Klinger, T. (2022). Identifying dietary preferences in breeding Pigeon Guillemot (*Cepphus columba*) using different methods. *Northwestern Naturalist*, *103*(1), 42–50. https://doi.org/10.1898/1051-1733-103.1.42

Burger, A. E., & Powell, D. W. (1990). Diving depths and diet of Cassin's Auklet at Reef Island, British Columbia. Canadian Journal of Zoology, 68(7), 1572–1577. https://doi.org/10.1139/z90-232

Cai, W., et al. (2014). Increasing frequency of extreme El Niño events due to greenhouse warming. Nature Climate Change 4:111–116.

Cane, M. A., Clement, A. C., Kaplan, A., Kushnir, Y., Pozdnyakov, D., Seager, R., Zebiak, S. E., & Murtugudde, R. (1997). Twentieth-Century sea surface temperature trends. Science, 275(5302), 957–960. https://doi.org/10.1126/science.275.5302.957

Carroll, M., Butler, A., Owen, E., Ewing, S., Cole, T., Green, J., Soanes, L., Arnould, J., Newton, S., Baer, J., Daunt, F., Wanless, S., Newell, M., Robertson, G., Mavor, R., & Bolton, M. (2015). Effects of sea temperature and stratification changes on seabird breeding success. *Climate Research*, 66(1), 75–89. https://doi.org/10.3354/cr01332

Chenillat, F., Rivière, P., Capet, X., Di Lorenzo, E., & Blanke, B. (2012). North Pacific Gyre Oscillation modulates seasonal timing and ecosystem functioning in the California Current upwelling system. Geophysical Research Letters, 39(1). https://doi.org/10.1029/2011GL049966

Converse, S. J., Royle, J. A., Adler, P. H., Urbanek, R. P., & Barzen, J. A. (2012). A hierarchical nest survival model integrating incomplete temporally varying covariates. *Ecology and Evolution*, 3(13), 4439–4447. https://doi.org/10.1002/ece3.822

Croxall, J. P., Butchart, S. H. M., Lascelles, B., Stattersfield, A. J., Sullivan, B., Symes, A., & Taylor, P. (2012). Seabird conservation status, threats and priority actions: a global assessment. Bird Conservation International, 22(1), 1–34. https://doi.org/10.1017/S0959270912000020

Cury, P. M., Boyd, I. L., Bonhommeau, S., Anker-Nilssen, T., Crawford, R. J. M., Furness, R. W., Mills, J. A., Murphy, E. J., Österblom, H., Paleczny, M., Piatt, J. F., Roux, J.-P., Shannon, L., & Sydeman, W. J. (2011). Global seabird response to forage fish depletion—one-third for the birds. *Science*, *334*(6063), 1703–1706. https://doi.org/10.1126/science.1212928

De Forest, L. G., & Busby, M. S. (2006). Development of larval and early juvenile penpoint gunnel (Apodichthys flavidus) (family: Pholidae). Fish. Bull. 104:476-481.

Di Lorenzo, E., & Mantua, N. (2016). Multi-year persistence of the 2014/15 North Pacific marine heatwave. Nature Climate Change, 6(11), 1042–1047. https://doi.org/10.1038/nclimate3082

Di Lorenzo E., Schneider N., Cobb K. M., Chhak, K, Franks P. J. S., Miller A. J., McWilliams J. C., Bograd S. J., Arango H., Curchister E., Powell T. M. & Rivere P. (2008). North Pacific Gyre Oscillation links ocean climate and ecosystem change. *Geophys. Res. Lett*., 35, L08607, doi:10.1029/2007GL032838.

Emms, S. K., & Verbeek, N. A. M. (1991). Brood size, food provisioning and chick growth in the Pigeon Guillemot Cepphus columba. The Condor, 93(4), 943. https://doi.org/10.2307/3247729

Ewins, P. J. (2020). Pigeon Guillemot (*Cepphus columba*), version 1.0. *Birds of the World* (A. F. Poole and F. B. Gill, Editors). Cornell Lab of Ornithology, Ithaca, NY, USA. https://doi-org.offcampus.lib.washington.edu/10.2173/bow.piggui.01

Frederiksen, M., Edwards, M., Mavor, R., & Wanless, S. (2007). Regional and annual variation in black-legged kittiwake breeding productivity is related to sea surface temperature. *Marine Ecology Progress Series*, 350, 137–143. https://doi.org/10.3354/meps07126

Furness, R. & Camphuysen, K. (1997). Seabirds as monitors of the marine environment. ICES Journal of Marine Science, 54(4), 726–737. https://doi.org/10.1006/jmsc.1997.0243

Golet, G. H., Kuletz, K. J., Roby, D. D., & Irons, D. B. (2000). Adult prey choice affects chick growth and reproductive success in Pigeon Guillemots. *The Auk*, 117(1), 82–91. https://doi.org/10.1093/auk/117.1.82

Grémillet, D., & Boulinier, T. (2009). Spatial ecology and conservation of seabirds facing global climate change: A review. Marine Ecology Progress Series, 391, 121–137. https://doi.org/10.3354/meps08212

Grémillet, D., Lewis, S., Drapeau, L., Van Der Lingen, C. D., Huggett, J. A., Coetzee, J. C., Verheye, H. M., Daunt, F., Wanless, S., & Ryan, P. G. (2008). Spatial match–mismatch in the Benguela upwelling zone: Should we expect chlorophyll and sea-surface temperature to predict marine predator distributions? *Journal of Applied Ecology*, 45(2), 610–621. https://doi.org/10.1111/j.1365-2664.2007.01447.x

Hayward, T. L. (1997). Pacific Ocean climate change: atmospheric forcing, ocean circulation and ecosystem response. Trends in Ecology & Evolution, 12(4), 150–154. https://doi.org/10.1016/S0169-5347(97)01002-1

Huot, Y., Babin, M., Bruyant, F., Grob, C., Twardowski, M. S., & Claustre, H. (2007). Does chlorophyll a provide the best index of phytoplankton biomass for primary productivity studies? Biogeosciences discussions, 4(2), 707-745.

Jeffreys, H. (1961). Theory of probability, third edition. Oxford University Press, Oxford, UK.

Joh, Y., & Di Lorenzo, E. (2017). Increasing coupling between NPGO and PDO leads to prolonged marine heatwaves in the Northeast Pacific: marine heatwaves in Northeast Pacific. Geophysical Research Letters, 44. https://doi.org/10.1002/2017GL075930

Johns, M., & Warzybok, P. (2022). Northward migration, molting locations, and winter residency of California breeding Pigeon Guillemots *Cepphus columba*. Marine Ecology Progress Series, 701, 133–143. https://doi.org/10.3354/meps14194

Kuo, L., & Mallick, B. (1998). Variable selection for regression models. Sankhyā: The Indian Journal of Statistics, Series B (1960-2002), 60(1), 65–81.

Link, W. A., & Barker, R. J. (2006). Model weights and the foundations of multimodel inference. *Ecology*, *87*(10), 2626–2635. https://doi.org/10.1890/0012-9658(2006)87[2626:MWATFO]2.0.CO;2

Litzow, M. A., Piatt, J. F., Abookire, A. A., & Robards, M. D. (2004). Energy density and variability in abundance of Pigeon Guillemot prey: support for the quality–variability trade-off hypothesis. Journal of Animal Ecology, 73, 1149–1156.

Litzow, M. A., Piatt, J. F., Prichard, A. K., & Roby, D. D. (2002). Response of Pigeon Guillemots to variable abundance of high-lipid and low-lipid prey. *Oecologia*, *132*(2), 286–295. https://doi.org/10.1007/s00442-002-0945-1

Litzow, M. A., & Piatt, J. F. (2003). Variance in prey abundance influences time budgets of breeding seabirds: evidence from Pigeon Guillemots *Cepphus columba*. *Journal of Avian Biology*, *34*(1), 54–64. https://doi.org/10.1034/j.1600-048X.2003.02995.x

Lu, G (2023). British Columbia lighthouse sea-surface temperature and salinity data (Pacific), 1914-present. Fisheries and Oceans Canada.

Mackas, D. L., Batten, S., & Trudel, M. (2007). Effects on zooplankton of a warmer ocean: recent evidence from the Northeast Pacific. Progress in Oceanography, 75(2), 223–252. https://doi.org/10.1016/j.pocean.2007.08.010

Mallory, M. L., Robinson, S. A., Hebert, C. E., & Forbes, M. R. (2010). Seabirds as indicators of aquatic ecosystem conditions: a case for gathering multiple proxies of seabird health. *Marine Pollution Bulletin*, *60*(1), 7–12. https://doi.org/10.1016/j.marpolbul.2009.08.024

Mantua, N.J. (1999). The Pacific Decadal Oscillation. A brief overview for non-specialists, Encyclopedia of Environmental Change.

Mantua, N. J., & Hare, S. R. (2002). The Pacific Decadal Oscillation. Journal of Oceanography, 58(1), 35–44. https://doi.org/10.1023/A:1015820616384

McGowan, J. A., Cayan, D. R., & Dorman, L. M. (1998). Climate-ocean variability and ecosystem response in the Northeast Pacific. Science, 281(5374), 210–217. https://doi.org/10.1126/science.281.5374.210

NASA Goddard Space Flight Center, Ocean Ecology Laboratory, Ocean Biology Processing Group (2018). Chlorophyll-a, Orbview-2 SeaWiFS, R2018.0, 0.1°, Global, 1997-2010 (Monthly Composite). NASA/GSFC/OBPG. https://dx.doi.org/10.5067/ORBVIEW-2/SEAWIFS/L3M/CHL/2018

NASA Goddard Space Flight Center, Ocean Ecology Laboratory, Ocean Biology Processing Group (2022). Chlorophyll-a, Aqua MODIS, NPP, L3SMI, Global, 4km, Science Quality, 2003-present

(Monthly Composite). NOAA NMFS SWFSC ERD. https://dx.doi.org/10.5067/AQUA/MODIS/L3M/CHL/2018

Parsons, M., Mitchell, I., Butler, A., Ratcliffe, N., Frederiksen, M., Foster, S., & Reid, J. B. (2008). Seabirds as indicators of the marine environment. ICES Journal of Marine Science, 65(8), 1520–1526. https://doi.org/10.1093/icesjms/fsn155

Pearson, S.F. and Hamel, N.J. 2013. Marine and terrestrial bird indicators for Puget Sound. Washington Department of Fish and Wildlife and Puget Sound Partnership, Olympia, WA, 55 pp.

Piatt, J. F., Harding, A. M. A., Shultz, M., Speckman, S. G., Pelt, T. I. van, Drew, G. S., & Kettle, A. B. (2007). Seabirds as indicators of marine food supplies: Cairns revisited. *Marine Ecology Progress Series*, *352*, 221–234. https://doi.org/10.3354/meps07078

Pinaud, D., & Weimerskirch, H. (2007). At-sea distribution and scale-dependent foraging behaviour of petrels and albatrosses: A comparative study. Journal of Animal Ecology, 76(1), 9–19. https://doi.org/10.1111/j.1365-2656.2006.01186.x

Plummer, M. (2003). JAGS: A program for analysis of Bayesian graphical models using Gibbs sampling. Proceedings of the 3rd International Workshop on Distributed Statistical Computing (DSC 2003), Vienna, 20-22 March 2003, 1-10.

R Core Team (2021). R: a language and environment for statistical computing. R Foundation for Statistical Computing, Vienna, Austria. https://www.R-project.org/.

Sandvik, H., Erikstad, K. E., & Sæther, B.-E. (2012). Climate affects seabird population dynamics both via reproduction and adult survival. Marine Ecology Progress Series, 454, 273–284. https://doi.org/10.3354/meps09558

Santo, T. L. D., & Nelson, S. K. (n.d.). Comparative reproductive ecology of the Auks (Family Alcidae) with emphasis on the Marbled Murrelet. USDA Forest Service Gen. Tech. Rep. PSW-152.

Seager, R., Cane, M., Henderson, N., Lee, D.-E., Abernathey, R., & Zhang, H. (2019). Strengthening tropical Pacific zonal sea surface temperature gradient consistent with rising greenhouse gases. Nature Climate Change, 9(7), 517–522. https://doi.org/10.1038/s41558-019-0505-x

Shimabukuro, U., Takahashi, A., Okado, J., Kokubun, N., Thiebot, J.-B., Will, A., Watanuki, Y., Addison, B., Hatch, S. A., Hipfner, J. M., Slater, L., Drummond, B. A., & Kitaysky, A. S. (2023). Across the North Pacific, dietary-induced stress of breeding Rhinoceros Auklets increases with high summer Pacific Decadal Oscillation index. *Marine Ecology Progress Series*, 708, 177–189. https://doi.org/10.3354/meps14276

Smith, D. H. V., Converse, S. J., Gibson, K. W., Moehrenschlager, A., Link, W. A., Olsen, G. H., et al. (2011). Decision analysis for conservation breeding: maximizing production for reintroduction of whooping cranes. Journal of Wildlife Management, 75, 501–505.

Studwell, A. J., Hines, E., Elliott, M. L., Howar, J., Holzman, B., Nur, N., & Jahncke, J. (2017). Modeling nonresident seabird foraging distributions to inform ocean zoning in central California. *PLOS ONE*, 12(1), e0169517. https://doi.org/10.1371/journal.pone.0169517

Thompson, S. A., Sydeman, W. J., Santora, J. A., Morgan, K. H., Crawford, W., & Burrows, M. T. (2012). Phenology of pelagic seabird abundance relative to marine climate change in the Alaska Gyre. Marine Ecology Progress Series, 454, 159–170. https://doi.org/10.3354/meps09598

Timmermann, A., Oberhuber, J., Bacher, A., Esch, M., Latif, M., & Roeckner, E. (1999). Increased El Niño frequency in a climate model forced by future greenhouse warming. Nature, 398(6729), 694–697. https://doi.org/10.1038/19505

Vandenbosch, R. (2000). Effects of ENSO and PDO events on seabird populations as revealed by Christmas Bird Count data. *Waterbirds: The International Journal of Waterbird Biology*, 23(3), 416–422. https://doi.org/10.2307/1522178

Wagner, E. L., Pearson, S. F., Good, T. P., Hodum, P. J., Buhle, E. R., & Schrimpf, M. B. (2023). Resilience to a severe marine heatwave at two Pacific seabird colonies. Marine Ecology Progress Series, HEAT. https://doi.org/10.3354/meps14222

Warlick, A. (2022). Understanding the effects of environmental variability on demography in species with complex life histories through integrated population modeling. ProQuest Dissertations Publishing.

Watanabe, S. (2013). A widely applicable Bayesian information criterion. Journal of Machine Learning Research, 14, 867–897.

Wilson, U. W. (2005). The effect of the 1997-1998 El Niño on Rhinoceros Auklets on Protection Island, Washington. *The Condor*, *107*(2), 462–468. https://doi.org/10.1650/7574

Zhang, Y., Wallace, J. M., & Battisti, D. S. (1997). ENSO-like interdecadal variability: 1900–93. Journal of Climate, 10(5), 1004–1020. https://doi.org/10.1175/1520-0442(1997)010<1004:ELIV>2.0.CO;2

1.7 FIGURES AND TABLES

Table 1.1 Summary of Pigeon Guillemot nesting outcomes from nesting boxes located at Protection Island, Washington, USA, from 1996 – 2013 and 2022 – 2023. Data include the number of nests that were monitored in nest boxes (excluding five with data entry errors), the number of nests that were censored from the analysis because monitoring terminated while there were still chicks in the nestboxes, the number of nests that failed (i.e., fledged no chicks), the number that fledged one chick, and the number that fledged two chicks. See text for specifics on nest monitoring methods. Note that in all years, the number of nest boxes available on the island exceeded the number of nests monitored.

Year	Nests Monitored	Nests Censored[a]	Nest Failures	Fledged One Chick	Fledged Two Chicks
1996	18	6	3	5	4
1997	29	3	9	13	4
1998	28	0	20	2	6
1999	30	0	9	17	4
2000	36	0	10	19	7
2001	38	0	5	21	12
2002	39	0	10	21	8
2003	36	0	19	13	4
2004	36	0	17	13	6
2005	33	0	15	16	2
2006	35	0	13	19	3
2007	37	0	17	17	3
2008	35	0	14	13	8
2009	38	1	11	19	7
2010	37	0	12	19	6
2011	22	0	7	11	4
2012	25	0	9	12	4
2013	23	0	4	16	3
2022	17	0	9	8	0
2023	23	0	16	5	2
Total	615	10	229	279	97

[a]Nests were censored if guillemot chicks were present in the nest through the final observation, which prevented determiniation of nest fate.

Table 1.2 Model selection results for selection of the best temporal scale for each of the four oceanographic covariates used to predict Pigeon Guillemot breeding outcomes at Protection Island, Washington, USA. Sea surface temperature (SST), chlorophyll-a concentration (CHLa), the Pacific Decadal Oscillation (PDO), and the North Pacific Gyre Oscillation (NPGO) were each identified as potential predictors of breeding success. At the first stage of model selection, we iterated through each time scale (see text) for each parameter (ϕ and γ) while keeping a null model structure for the other parameter, i.e., for each parameter, we fit 20 models (4 covariates by 5 time scales). We retained the time scale for each covariate that performed best in terms of ΔWAIC for each of the parameters. Best performing covariates are bolded.

Parameter	**Covariate**	**Time Scale**				
		YearEarly	**YearLate**	**Winter**	**LateWinter**	**Breed**
ϕ	SST	0.4	0.1	0.3	0.2	**0.0**
	CHLa	0.5	0.2	0.2	**0.0**	0.7
	NPGO	**0.0**	0.3	0.4	0.6	1.3
	PDO	0.1	0.4	0.3	0.2	**0.0**
γ	SST	**0.0**	0.4	0.4	0.5	0.2
	CHLa	0.7	0.3	**0.0**	0.2	0.7
	NPGO	0.3	1.9	**0.0**	1.4	2.5
	PDO	1.5	0.9	0.2	**0.0**	2.0

Table 1.3 Model selection results for the models with at least 1% of the total weight, describing relationships between oceanographic conditions and Pigeon Guillemot nesting outcomes at Protection Island, Washington, USA, from 1996 – 2013. Model weights are the proportion of 50,000 Markov chain Monte Carlo iterations in which a given model was selected using an indicator variable approach (see text for description of method). Each model consists of a covariate structure on two response variables, including ϕ_i, the probability that nest *i* produces at least one fledgling, and γ_i, the probability that nest *i* produces two fledglings, conditional on producing at least one. Covariates are described in Table 1.2. A random effect of year is also included, given as $\varepsilon^{\phi}_{t[i]}$, which is sampled from a normal distribution.

Model	Weight (%)
$logit(\phi_i) = \beta_0^{\phi} + \beta_1^{\phi} * NPGO.YearEarly_{t[i]} + \varepsilon^{\phi}_{t[i]}$ $logit(\gamma_i) = \beta_0^{\gamma} + \varepsilon^{\gamma}_{t[i]}$	32.26
$logit(\phi_i) = \beta_0^{\phi} + \varepsilon^{\phi}_{t[i]}$ $logit(\gamma_i) = \beta_0^{\gamma} + \varepsilon^{\gamma}_{t[i]}$	13.59
$logit(\phi_i) = \beta_0^{\phi} + \beta_1^{\phi} * NPGO.YearEarly_{t[i]} + \varepsilon^{\phi}_{t[i]}$ $logit(\gamma_i) = \beta_0^{\gamma} + \beta_1^{\gamma} * PDO.Winter_{t[i]} + \varepsilon^{\gamma}_{t[i]}$	8.82
$logit(\phi_i) = \beta_0^{\phi} + \beta_1^{\phi} * NPGO.YearEarly_{t[i]} + \varepsilon^{\phi}_{t[i]}$ $logit(\gamma_i) = \beta_0^{\gamma} + \beta_1^{\gamma} * NPGO.LateWinter_{t[i]} + \varepsilon^{\gamma}_{t[i]}$	6.82
$logit(\phi_i) = \beta_0^{\phi} + \beta_1^{\phi} * CHLa.LateWinter_{t[i]} + \varepsilon^{\phi}_{t[i]}$ $logit(\gamma_i) = \beta_0^{\gamma} + \varepsilon^{\gamma}_{t[i]}$	3.12
$logit(\phi_i) = \beta_0^{\phi} + \beta_1^{\phi} * CHLa.LateWinter_{t[i]} + \beta_2^{\phi} * NPGO.YearEarly_{t[i]} + \varepsilon^{\phi}_{t[i]}$ $logit(\gamma_i) = \beta_0^{\gamma} + \varepsilon^{\gamma}_{t[i]}$	3.11
$logit(\phi_i) = \beta_0^{\phi} + \varepsilon^{\phi}_{t[i]}$ $logit(\gamma_i) = \beta_0^{\gamma} + \beta_1^{\gamma} * PDO.Winter_{t[i]} + \varepsilon^{\gamma}_{t[i]}$	3.09
$logit(\phi_i) = \beta_0^{\phi} + \beta_1^{\phi} * NPGO.YearEarly_{t[i]} + \varepsilon^{\phi}_{t[i]}$ $logit(\gamma_i) = \beta_0^{\gamma} + \beta_1^{\gamma} * CHLa.LateWinter_{t[i]} + \varepsilon^{\gamma}_{t[i]}$	2.78

$logit(\phi_i) = \beta_0^{\phi} + \varepsilon_{t[i]}^{\phi}$ $logit(\gamma_i) = \beta_0^{\gamma} + \beta_1^{\gamma} * NPGO.LateWinter_{t[i]} + \varepsilon_{t[i]}^{\gamma}$	2.52
$logit(\phi_i) = \beta_0^{\phi} + \beta_1^{\phi} * NPGO.YearEarly_{t[i]} + \varepsilon_{t[i]}^{\phi}$ $logit(\gamma_i) = \beta_0^{\gamma} + \beta_1^{\gamma} * SST.YearEarly_{t[i]} + \varepsilon_{t[i]}^{\gamma}$	2.07
$logit(\phi_i) = \beta_0^{\phi} + \beta_1^{\phi} * NPGO.YearEarly_{t} + \varepsilon_{t[i]}^{\phi}$ $logit(\gamma_i) = \beta_0^{\gamma} + \beta_1^{\gamma} * NPGO.LateWinter_{t[i]} + \beta_1^{\gamma} * PDO.Winter_{t[i]} + \varepsilon_{t[i]}^{\gamma}$	1.83
$logit(\phi_i) = \beta_0^{\phi} + \beta_1^{\phi} * NPGO.YearEarly_{t[i]} + \beta_2^{\phi} * PDO.Breed_{t[i]} + \varepsilon_{t[i]}^{\phi}$ $logit(\gamma_i) = \beta_0^{\gamma} + \varepsilon_{t[i]}^{\gamma}$	1.67
$logit(\phi_i) = \beta_0^{\phi} + \varepsilon_{t[i]}^{\phi}$ $logit(\gamma_i) = \beta_0^{\gamma} + \beta_1^{\gamma} * CHLa.LateWinter_{t[i]} + \varepsilon_{t[i]}^{\gamma}$	1.07

Table 1.4 Model selection results for the four oceanographic covariates used to predict two parameters of Pigeon Guillemot breeding outcomes, ϕ, the probability that at nest produces at least one fledgling, and γ, the probability that a nest produces two fledglings, conditional on producing at least one. Covariates include sea surface temperature (SST), chlorophyll-a concentration (CHLa), the North Pacific Gyre Oscillation (NPGO), and the Pacific Decadal Oscillation (PDO). The posterior inclusion probability is the probability that the covariate will be included in the model, and the Bayes factor is the posterior odds ratio in favor of the set of models including the covariate versus the set of models not including the variable.

Parameter	Covariate	Posterior Inclusion Probability	Bayes Factor
ϕ	SST.Breed	0.03	0.04
	CHLa.LateWinter	0.13	0.15
	NPGO.YearEarly	0.68	2.14
	PDO.Breed	0.05	0.06
γ	SST.YearEarly	0.07	0.07
	CHLa.Winter	0.07	0.08
	NPGO.LateWinter	0.17	0.20
	PDO.Winter	0.20	0.25

Figure 1.1 Locations of occupied nest boxes on Protection Island in 2022. Boxes are marked with a yellow point. The boxes were placed in three distinct areas: Kanem Point (in the southwest of the island), mid-shore (on the central-southern coast of the island), and the marina, towards the east of the island. During the 1996-2013 monitoring period, the nest boxes were in and just to the southwest of the marina.

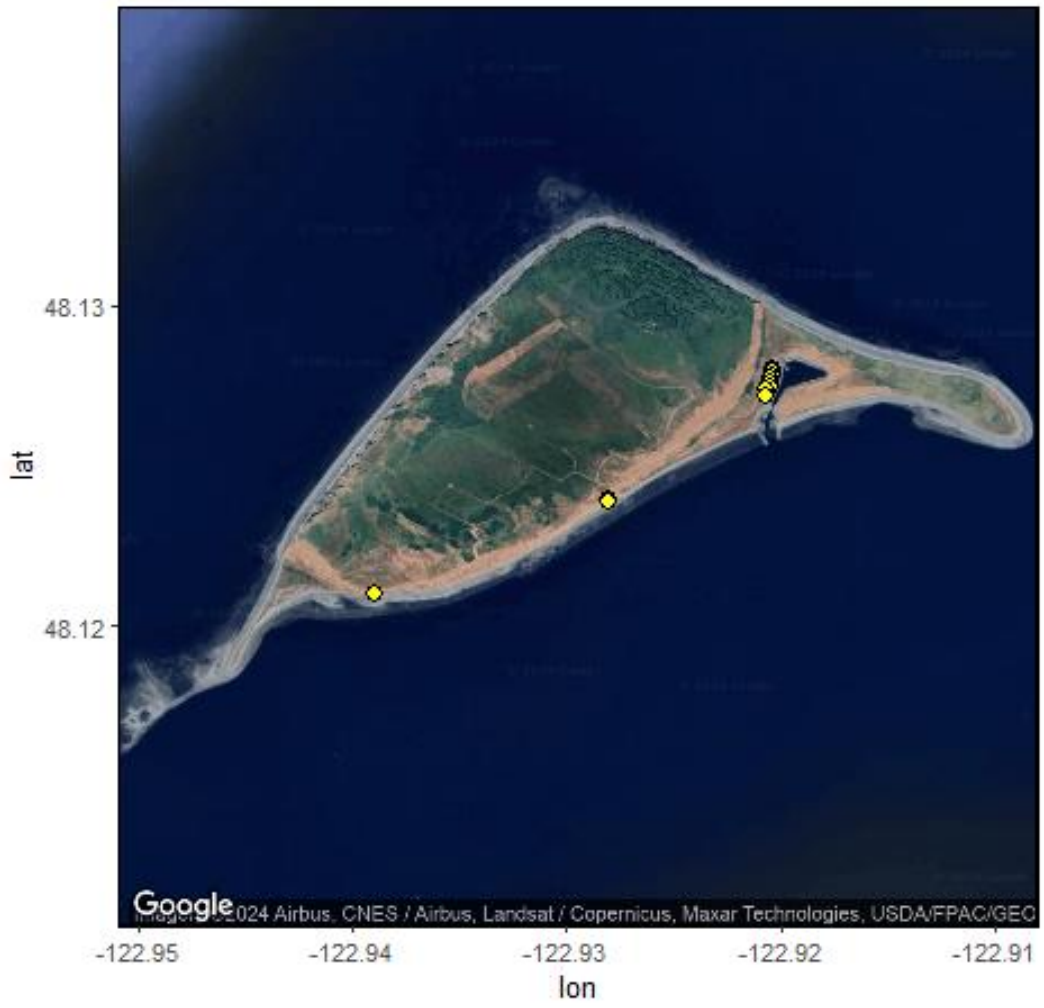

Figure 1.2 Locations of monitored nests on Protection Island in 2023. Boxes are marked with a yellow point. The boxes were placed in four distinct areas: Kanem Point (in the southwest of the island), mid-shore (on the central-southern coast of the island), the marina, and Violet Point (north of the marina along the north shore).

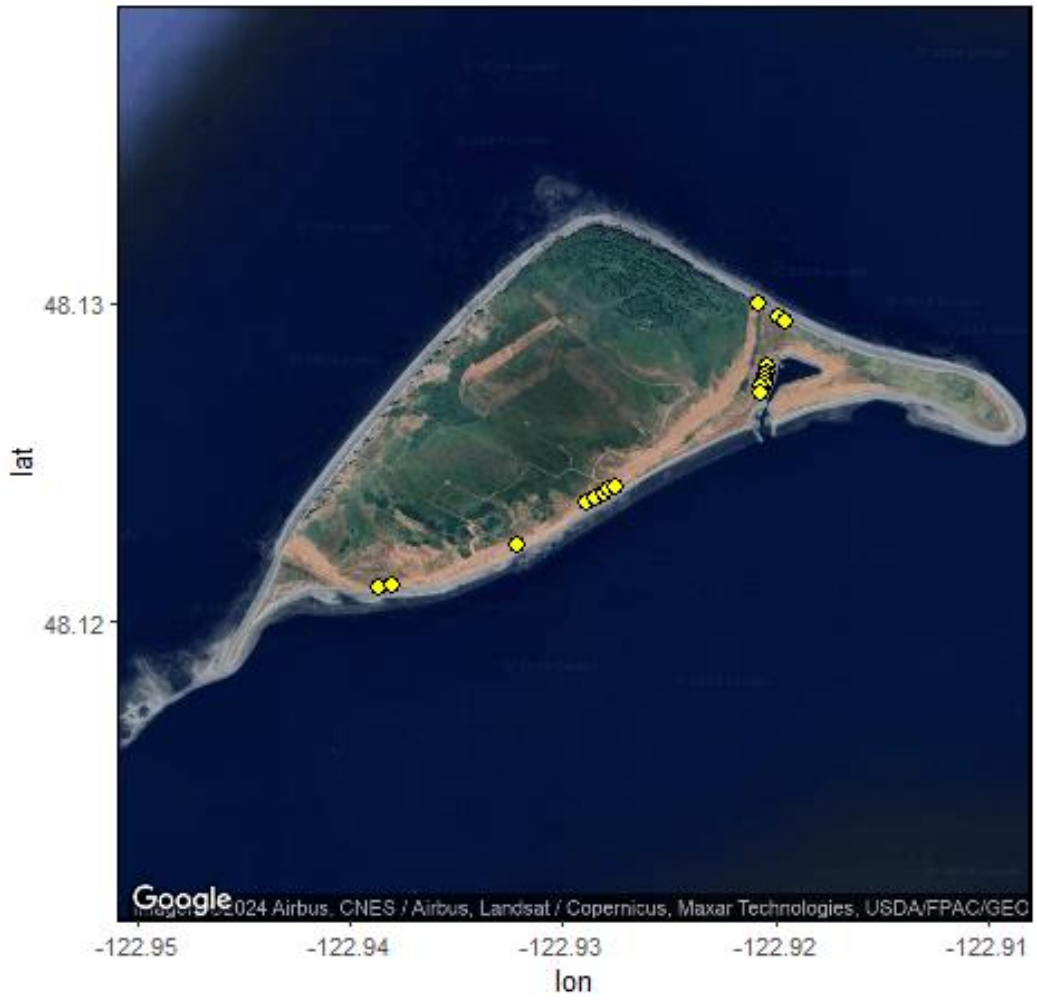

Figure 1.3 Pairwise correlation among all temporal windows for each covariate. Sea surface temperature (SST), chlorophyll-a concentration (CHLa), the North Pacific Gyre Oscillation (NPGO) index and the Pacific Decadal Oscillation (PDO) index were all broken into five alternative temporal windows each (YearEarly, YearLate, Winter, LateWinter, and Breed; see *Oceanographic Covariates*).

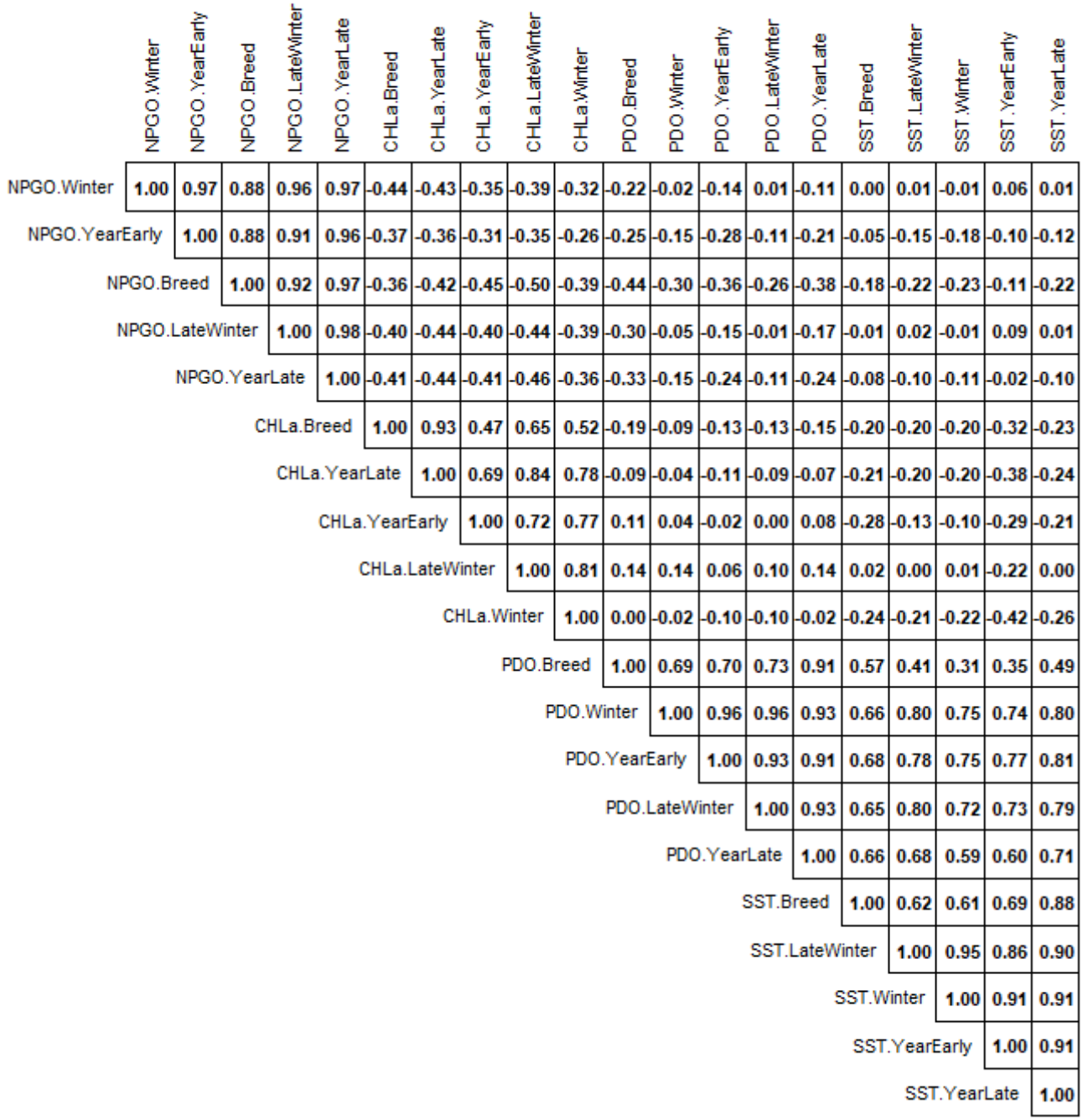

	NPGO.Winter	NPGO.YearEarly	NPGO.Breed	NPGO.LateWinter	NPGO.YearLate	CHLa.Breed	CHLa.YearLate	CHLa.YearEarly	CHLa.LateWinter	CHLa.Winter	PDO.Breed	PDO.Winter	PDO.YearEarly	PDO.LateWinter	PDO.YearLate	SST.Breed	SST.LateWinter	SST.Winter	SST.YearEarly	SST.YearLate
NPGO.Winter	1.00	0.97	0.88	0.96	0.97	-0.44	-0.43	-0.35	-0.39	-0.32	-0.22	-0.02	-0.14	0.01	-0.11	0.00	0.01	-0.01	0.06	0.01
NPGO.YearEarly		1.00	0.88	0.91	0.96	-0.37	-0.36	-0.31	-0.35	-0.26	-0.25	-0.15	-0.28	-0.11	-0.21	-0.05	-0.15	-0.18	-0.10	-0.12
NPGO.Breed			1.00	0.92	0.97	-0.36	-0.42	-0.45	-0.50	-0.39	-0.44	-0.30	-0.36	-0.26	-0.38	-0.18	-0.22	-0.23	-0.11	-0.22
NPGO.LateWinter				1.00	0.98	-0.40	-0.44	-0.40	-0.44	-0.39	-0.30	-0.05	-0.15	-0.01	-0.17	-0.01	0.02	-0.01	0.09	0.01
NPGO.YearLate					1.00	-0.41	-0.44	-0.41	-0.46	-0.36	-0.33	-0.15	-0.24	-0.11	-0.24	-0.08	-0.10	-0.11	-0.02	-0.10
CHLa.Breed						1.00	0.93	0.47	0.65	0.52	-0.19	-0.09	-0.13	-0.13	-0.15	-0.20	-0.20	-0.20	-0.32	-0.23
CHLa.YearLate							1.00	0.69	0.84	0.78	-0.09	-0.04	-0.11	-0.09	-0.07	-0.21	-0.20	-0.20	-0.38	-0.24
CHLa.YearEarly								1.00	0.72	0.77	0.11	0.04	-0.02	0.00	0.08	-0.28	-0.13	-0.10	-0.29	-0.21
CHLa.LateWinter									1.00	0.81	0.14	0.14	0.06	0.10	0.14	0.02	0.00	0.01	-0.22	0.00
CHLa.Winter										1.00	0.00	-0.02	-0.10	-0.10	-0.02	-0.24	-0.21	-0.22	-0.42	-0.26
PDO.Breed											1.00	0.69	0.70	0.73	0.91	0.57	0.41	0.31	0.35	0.49
PDO.Winter												1.00	0.96	0.96	0.93	0.66	0.80	0.75	0.74	0.80
PDO.YearEarly													1.00	0.93	0.91	0.68	0.78	0.75	0.77	0.81
PDO.LateWinter														1.00	0.93	0.65	0.80	0.72	0.73	0.79
PDO.YearLate															1.00	0.66	0.68	0.59	0.60	0.71
SST.Breed																1.00	0.62	0.61	0.69	0.88
SST.LateWinter																	1.00	0.95	0.86	0.90
SST.Winter																		1.00	0.91	0.91
SST.YearEarly																			1.00	0.91
SST.YearLate																				1.00

Figure 1.4 Estimated mean Pigeon Guillemot breeding success (ϕ; the probability of producing chicks) including 95% credible intervals of the best fit model, second best fit model, and the average between the two (see Table 1.3 for descriptions of the top two models).

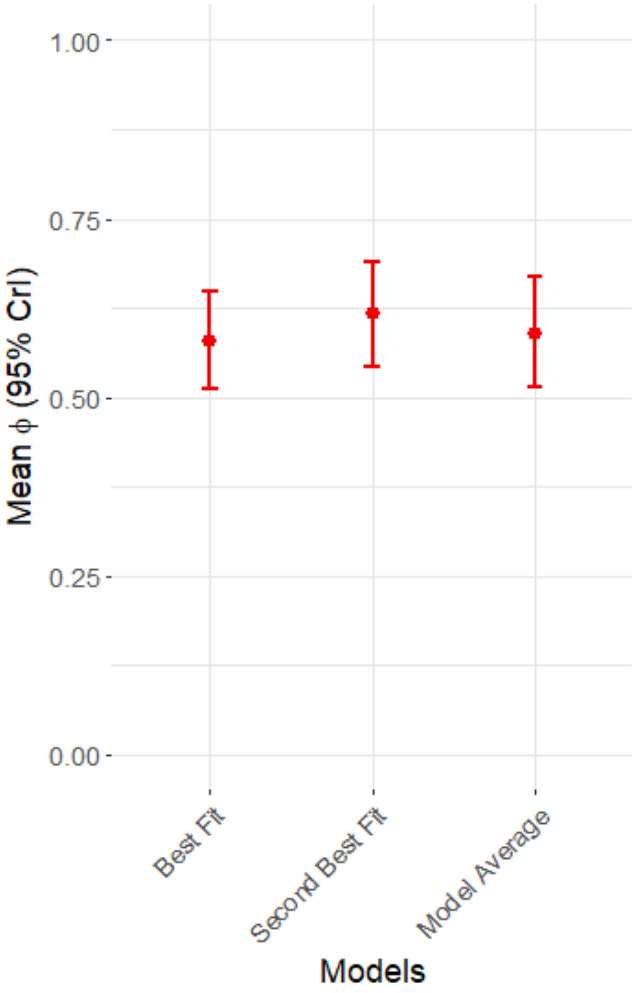

Figure 1.5 Estimated mean Pigeon Guillemot double fledging (γ) including 95% credible intervals of the best fit model, second best fit model, and the average between the two (see Table 1.3 for descriptions of the top two models).

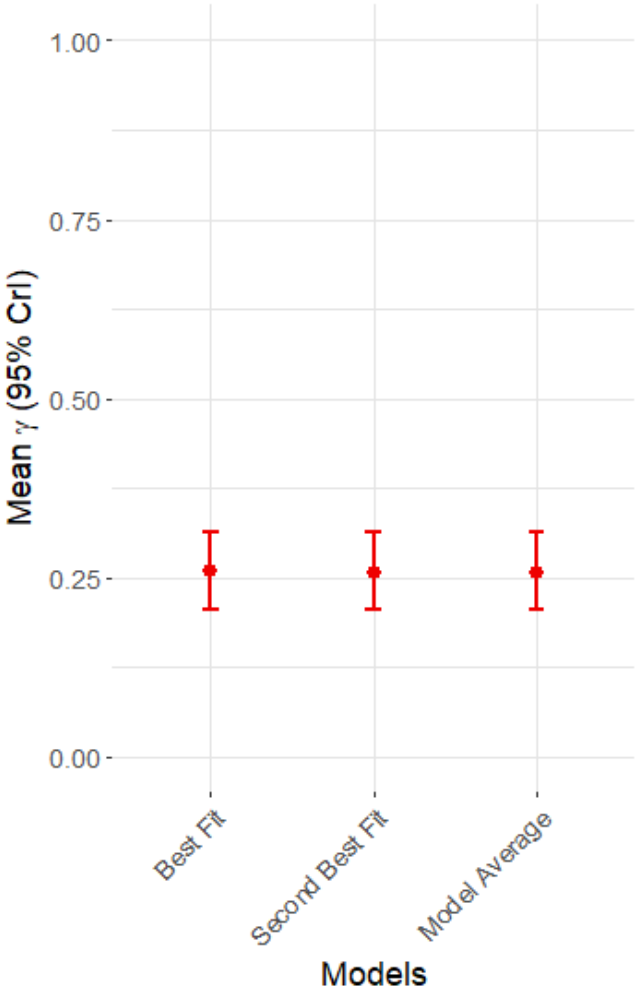

Figure 1.6 Predicted mean Pigeon Guillemot breeding success (ϕ) including 95% credible intervals across possible values of NPGO. Mean and credible intervals obtained from the best fit model (see Table 1.3 for description of the best fit model).

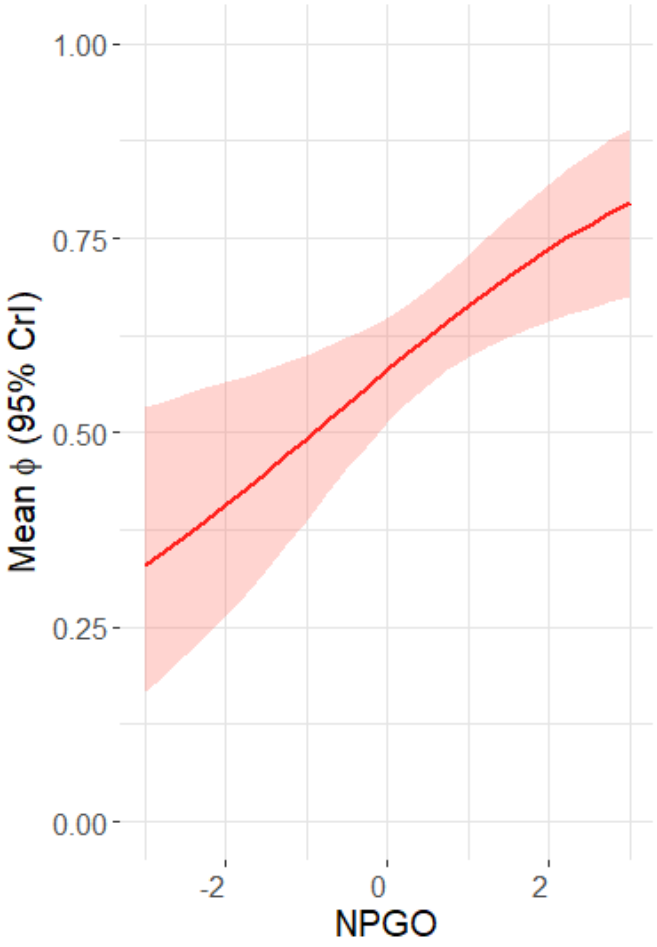

Chapter 2: Characterizing movements of breeding Pigeon Guillemots (*Cepphus columba*) and Rhinoceros Auklets (*Cerorhinca monocerata*)

Publication history: This study was co-authored with EL Wagner, SF Pearson, SM Thomas, and SJ Converse. At the time this thesis was published, this chapter was not in review with a journal.

2.1 ABSTRACT

Pigeon Guillemots (*Cepphus columba*) and Rhinoceros Auklets (*Cerorhinca monocerata*) are seabirds that have been identified as indicators of the health of Puget Sound, yet significant gaps still exist in our knowledge of their foraging behavior during the breeding season. In this study, we used GPS telemetry to track movements of these seabirds during the breeding season at Protection Island, Washington, USA, and we used hidden Markov modeling to classify behavioral states and estimate movement parameters, allowing us to expand on existing evidence for the substantially different foraging strategies of these two species. Pigeon Guillemots exhibited shorter and more range-limited movements to provision their young compared to Rhinoceros Auklets. However, foraging and resting states appeared to be difficult to distinguish in the models. Additional development of hidden Markov modeling is needed to more clearly distinguish behavioral states for these two species, which will allow for a greater understanding of their breeding and foraging ecology, along with the identification of key foraging areas.

2.2 INTRODUCTION

Seabirds depend on year-round access to marine foraging habitat, with greater energetic needs during months when they are provisioning young. Breeding seabirds are central-place foragers, making trips between foraging sites and breeding colonies to provision nestlings (Orians and Pearson, 1979; Bell, 1990), such that foraging habitat must be adequately close to nesting habitat to meet seabirds' energetic needs. Understanding how seabirds exploit distinct foraging and breeding habitat is necessary for addressing basic ecological questions, and for identifying foraging habitats around breeding colonies that are critical to protect. Understanding how seabirds meet their foraging habitat needs in particular can be

challenging, as foraging behavior can be difficult to observe directly, and can vary substantially, given differences in species physiology (Fromant et al., 2021), time budgets (Cairns et al., 1987; Ropert-Coudert et al., 2004), prey availability and distribution (Gaston et al., 2007; Elliott et al., 2008), and environmental conditions (Fromant et al., 2021).

To better understand how birds are using marine habitats to meet their life history needs, we can study their movements (Evans et al., 2013). In particular, we can use movement data to identify behavioral states – e.g., traveling, foraging, or nest and chick care. This requires, in addition to fine-scale movement data, some prior knowledge of the life histories of the target species and appropriate analytical methods. Methods to infer behavior from tracking data typically involve two steps. First, individuals are tracked using methods such as satellite telemetry (Stoneburner, 1982; Keating et al., 1991; Godley et al., 2008), radio-telemetry (Mech, 1967; Lee et al., 1985; Miller et al., 2005), or camera traps (Royle et al., 2013; Frey et al., 2017). The methods with which animals are tracked requires species-specific considerations to avoid impacting behavior (Wilson et al., 1997; Tudorache et al., 2014; van der Hoop et al., 2014). Seabirds are commonly tracked using VHF radio tags (Jodice and Collopy, 1999; Lamb et al., 2023), light-level geolocator tags (Weimerskirch and Wilson, 2000; Johns and Warzybok, 2022), or global positioning system (GPS) tags (Grémillet et al., 2004; Chimienti et al., 2017; Critchley et al., 2020). After obtaining tracking data, models describing the underlying factors that drive these observations are developed. A variety of modeling frameworks exist, including state-space models (Breed et al., 2012), change point analyses (Patel et al., 2015), and dynamic time warping (Cleasby et al., 2019). Hidden Markov models (HMMs) are a specific type of state-space models that can be particularly useful for understanding movement states (Zhang et al., 2019; Beumer et al., 2020). In movement ecology, HMMs are often used to delineate latent behavioral states and state transition probabilities through the analysis of time series of location data. Using HMMs to identify where specific behaviors (such as foraging) occur can contribute to animal conservation, as identifying where state-specific behaviors occur can help inform protection of critical habitat.

Pigeon Guillemots (*Cepphus columba;* hereafter, guillemots) and Rhinoceros Auklets (*Cerorhinca monocerata;* hereafter, auklets) are two seabirds that have been identified as indicators of marine ecosystem health in Puget Sound, Washington, USA (Pearson and Hamel, 2013). Both species are abundant on Protection Island in the Strait of Juan de Fuca, and while aspects of their foraging ecology have been described (Wilson and Manuwal, 1986; Thompson, 2005; Bishop et al., 2016; Buckner et al., 2022; Johns and Warzybok, 2022), little work has been done to explore fine-scale foraging behaviors, limiting our understanding of how they use their habitat and how much time is dedicated to different behaviors during the breeding season. They are central-place foragers during the breeding season but exhibit markedly different foraging and provisioning strategies. Breeding guillemots make many foraging trips throughout the day to provision young, and do not travel very far from their nests, coming back to land at dusk (Litzow et al., 2004; Johns and Warzybok, 2022). Conversely, auklets spend most of the day away from the colony and do not return to provision chicks until night, allowing them to travel much farther while foraging (Wilson, 1977). These patterns are observable when their movements are tracked and can be used to quantify movement parameters and classify patterns into distinct latent behavioral states, which can in turn be used to advance conservation and management goals.

In this study, we used HMMs to describe state-specific movements of guillemots and auklets during the breeding season at Protection Island, Washington, USA. We used GPS tags to track movements of these species during the breeding seasons of 2022 and 2023. We analyzed these data with discrete-time HMMs to classify their movement into stationary, transiting, and foraging states. Our results generally confirmed the substantially different foraging and provisioning strategies of these species, but models performed poorly for distinguishing stationary and foraging states. With additional development, models of this kind have the potential to assist with the identification of critical seabird foraging habitat in the region, and we suggest future steps to improve model performance.

2.3 METHODS

2.3.1 System and Study Species

This study took place at Protection Island in Jefferson County, Washington, USA (Figure 2.1). Protection Island is located at the eastern end of the Strait of Juan de Fuca where it meets Puget Sound. The island has a land area of 153 hectares and is closed to the public, minimizing risk of human disturbance to the study area. The island is owned primarily by the US Fish and Wildlife Service and is designated as Protection Island National Wildlife Refuge, though one portion of the island is owned by Washington Department of Fish and Wildlife and is designated as the Zella M. Schultz Seabird Sanctuary. Protection Island has an estimated guillemot population size of 1,200 individuals (S. Thomas, USFWS, 2023, unpublished data), and an estimated auklet population size of 36,152 individuals (Pearson et al., 2013).

Both guillemots and auklets are members of the auk family (*Alcidae*). Guillemots typically feed on demersal, non-schooling fish species such as gunnel (*Pholis* spp.), sculpin (*Leptocottus* spp.), and rockfish (*Sebastes* spp.), but are also known to selectively forage for higher-lipid schooling species including Pacific sand lance (*Ammodytes hexapterus*) and Pacific herring (*Clupea pallasii*) (Golet et al., 2000; Litzow and Piatt, 2003; Buckner et al., 2022). They provision young many times throughout the day, and their provisioning rates are largely determined by the quality and abundance of their prey (Litzow and Piatt, 2003). Their preference for demersal species and their frequent provisioning suggests that they forage in nearshore areas and do not travel far from their nests (Litzow et al., 2004; Johns and Warzybok, 2022). They primarily forage in waters < 20 m deep but can make dives up to 50 m deep (Kuletz, 1998).

Auklet diets during the breeding season consist primarily of higher-lipid schooling fish including Pacific sandlance, Pacific herring, and rockfish (Vermeer and Devito, 1986; Beaubier and Hipfner, 2012), but may also include northern anchovy (*Engraulis mordax*) and smelt (*Osmeridae* spp.) (Wagner et al.,

2023). Auklets spend the majority of their day foraging at sea and only return to their burrows at dusk, delivering at least one bill load per parent to chicks (Wilson, 1977), though they may increase provisioning frequency if available prey species are less calorically rich (Watanuki et al., 2022). Auklets at Protection Island typically forage within 40 km of their colony, with around 30 – 40% foraging within 17 km (Wahl and Speich, 1994). They dive to obtain prey at depths >20 m and frequent areas where tidal currents concentrate prey, particularly in Admiralty Inlet and the San Juan Channel (Wahl and Speich, 1994).

2.3.2 Data

2.3.2.1 GPS Tagging and Data Retrieval

GPS tags manufactured by PathTrack Ltd. (Otley, UK) were used for tracking guillemots and auklets. Tags weighed < 5g, which is less than 2% of adult body weight of both guillemots and auklets, a threshold necessary to minimize negative impacts on birds (Sun et al., 2020). Eight tags were attached to each species in 2022. In 2023, eight tags were attached to auklets and seven to guillemots. Tags were attached in mid-June to early July during late incubation and chick provisioning. Guillemots were captured in nest boxes as part of a larger nest success study. Auklets were captured by hand at burrow openings as they returned at dusk. Because auklets were caught outside their burrows, they could not be tracked to a specific burrow, but because they arrived with bill-loads of fish, we inferred that they were provisioning chicks.

Tags were affixed to feathers on birds' lower back using waterproof Tesa tape (Wilson et al., 1997), manufactured by Tesa SE (Hamburg, Germany). Three to four strips of tape, each approximately 3 inches long, were slipped under birds' feathers with the adhesive side facing up. The tag was placed on top of the feathers above the tape, and the tape was then wrapped around the tag. Cyanoacrylate glue was added to the edges of the tape and allowed to dry before the bird was released.

Base stations were used to collect data from tags via a UHF signal when individuals were in range of the station. One base station was used in 2022 (Figure 2.2) and an additional base station was added in 2023 to maximize data reception (Figure 2.3). Tags were programmed to record individuals' locations every 15 minutes. In 2022 we programmed tags to attempt communication with the base station every 30 minutes but found this to be too infrequent, so in 2023 we changed this to five minutes. Data were downloaded from base stations every week.

2.3.2.2 Data Processing and Imputation

Tracking data were obtained from base stations using PathTrack Ltd. software (V2.35). Temporal gaps in the data were present and were primarily due to tags being unable to communicate with satellites, likely while individuals were in nest boxes or burrows. These gaps were too large to be able to consistently derive movement parameters between each step for the HMM (see *Movement Parameters*). We therefore imputed missing values using the multiple imputation procedure in the crawlWrap function from the momentuHMM package (version 2.0.0; McClintock and Michelot 2018). This procedure involves two steps (McClintock, 2017). First, the function repeatedly fits a single-state movement model, specifically a continuous time correlated random walk (Johnson et al. 2008), which can account for temporal irregularity in the data. Then, it fits an HMM to the *n* regularized tracks, and pools these estimates into a final track that accounts for uncertainty (Nakagawa and Freckleton, 2008; McClintock, 2017). We converted our data to UTM coordinates as required by the function, and imputed data at 15-minute intervals.

2.3.3 Movement Analysis

2.3.3.1 Movement Parameters

We used HMMs to classify movement states of breeding guillemots and auklets on Protection Island, which relied on movement parameters defined in the observation process. First, we used step length (the distance between two consecutive points in meters), defined as

$$L_t = \sqrt{(X_{t+1} - X_t)^2 + (Y_{t+1} - Y_t)^2}$$

where L_t is the step length between two consecutive time points, *t* and *t* + 1, and *X* and *Y* are location coordinates. We also used turn angle (the change in direction between two consecutive points), defined as

$$\Psi_t = tan^{-1}\left(\frac{Y_{t+1} - Y_t}{X_{t+1} - X_t}\right)$$

where Ψ_t is the turn angle between two consecutive points at time *t.* We selected commonly used distributions to model these parameters. We used a gamma distribution to describe step length (Saldanha et al., 2023; Pattison et al., 2022), parameterized based on the mean and standard deviation of step length, and a von Mises distribution for turn angle (Pattison et al., 2022; Zucchini et al., 2017), such that

$$L_t \mid (S_t = s) \sim gamma(\theta_s, \sigma_s)$$

$$\Psi_t \mid (S_t = s) \sim von\ Mises(\mu_s, \kappa_s)$$

where $\{S_t = s\}$ denotes state *s* at time *t,* L_t is the step length at time *t* conditional on the state, θ_s is the mean of the step length distribution given state *s,* σ_s is the standard deviation of the step length distribution given state *s,* Ψ_t is the turn angle at time *t,* μ_s is the mean of the turn angle distribution, and κ_s is the concentration (precision) of the turn angle distribution.

Initial values were necessary to estimate the parameters of the gamma and von Mises distributions for each of three states of interest – stationary, transiting, and foraging – for each species. Therefore, we specified initial values for the mean and standard deviation of the gamma distribution for each of these three states. We fixed the mean turn angle in the von Mises distribution to 0, implying short-term directional persistence between steps, and we specified initial values for concentration of turn angle for each of three states. We plotted a histogram of step lengths to visualize how they were distributed and to explore values to choose for parameterization (Michelot and Langrock, 2023). Given expectations that step lengths while resting, transiting, and foraging would be very small, long, and intermediate, respectively, we iteratively explored sets of initial values, assessed model fit using AIC, and visually

inspected plots of state sequences until settling on a final set of initial values. Because we only needed to specify concentration for turn angle, and because this is less interpretable from a histogram, we used an intuitive prior belief of how the concentration of turn angles in different states may appear. We used the same iterative exploration process to find initial values for turn angle, with the assumption that resting, transiting, and foraging states would yield very high, intermediate, and very low turn angle concentrations, respectively.

2.3.3.2 Hidden Markov Models

We used HMMs to classify guillemot and auklet movements into resting, transiting, and foraging states. Switches between states were modeled as a first-order Markov process, with a conditional distribution assigned to the latent state variable S_t such that

$$S_t|(\gamma, S_{t-1} = s) \sim Categorical(\gamma_{s,R}, \gamma_{s,T}, \gamma_{s,F})$$

where for *s, s'* ∈ {*R, T, F*} (i.e., resting, transiting, and foraging), $\gamma_{s,s'}$ is the probability of transitioning from state *s* at time *t*-1 to state *s'* at time *t*. The observation process was modeled as a bi-dimensional series of step lengths and angles, such that

$$f_s(X_t) = (f(L_t \mid S_t = s), f(\Psi_t \mid S_t = s))$$

where each observation *X* at time *t* consists of an associated step length and turn angle and is conditional on the underlying state.

The state process of the HMM is defined by three parameters: (1) π, an initial distribution, defined as

$$\pi = (P(S_1 = x), P(S_1 = y), P(S_1 = z))$$

(2) *A*, a transition probability matrix, defined as

$$A = \begin{bmatrix} \gamma_{1,1} & \gamma_{1,2} & \gamma_{1,3} \\ \gamma_{2,1} & \gamma_{2,2} & \gamma_{2,3} \\ \gamma_{3,1} & \gamma_{3,2} & \gamma_{3,3} \end{bmatrix}$$

and (3) an observation probability matrix *B*, defined as

$$B = \begin{bmatrix} f(X_1 = x_1 | S_t = R) & 0 & 0 \\ 0 & f(X_1 = x_1 | S_t = T) & 0 \\ 0 & 0 & f(X_1 = x_1 | S_t = F) \end{bmatrix}$$

where each observation *X* is conditional on its respective state. Finally, the likelihood function ($\mathcal{L}$) of the HMM is defined as

$$\mathcal{L} = P(O|\pi, A, B) = \sum_{s=1}^{3} \alpha_{s,T}$$

where $\alpha_{s,T}$ represents the probability of the entire observation sequence *O* ending in state *s* at time *t* given π, *A*, and *B*.

We fit our HMM using the fitHMM function in the momentuHMM package (version 2.0.0; McClintock and Michelot 2018) in R (version 4.3.3). The model was fitted by numerically maximizing the likelihood using a Newton-type optimization algorithm, and each state was modeled as a correlated random walk. We used the Viterbi algorithm to decode the most likely state sequence for each model, given the model fit, and from there calculated the amount of time spent in each state. We assessed model performance by first visually inspecting behavioral classification relative to known foraging behavior of the species. This was a useful first step in determining how accurate the models were in differentiating between behavioral states.

2.4 RESULTS

2.4.1 Tagging Data

Only six of the 15 tags attached to guillemots and seven of the 16 tags attached to auklets in 2022 and 2023 transmitted data of adequate quantity to allow for analysis (Table 2.1). Ten of the tags produced no data (i.e., may have fallen off immediately, otherwise malfunctioned, or never have come in range of a base station) and eight of the tags produced data of insufficient quality for analysis. Guillemot tracks consisted of t_{PIGU} = 3,264 locations with 3,179 missing records. Auklet tracks consisted of t_{RHAU} = 1,522

locations with 2,034 missing records (Table 2.1). In total, guillemot tags failed to capture approximately 46% of the potential data points during the duration tags were active, while auklet tags missed approximately 56% of potential points (Table 2.1). Most of the gaps in the data likely occurred when birds were nesting in boxes or burrows, inhibiting tags from communicating with satellites to record points. Of the 13 usable tracks, two auklet tracks (45653 and 45659) and one guillemot track (44372) could not be imputed by crawlWrap and were omitted from analysis. Therefore, results are based on five guillemot tracks and five auklet tracks.

2.4.2 Hidden Markov Model Analysis

2.4.2.1 Guillemots

Guillemot mean step lengths (in meters) for resting, transiting, and foraging states were 93 m (SD = 87 m), 903 m (SD = 1022 m), and 13 m (SD = 16 m), respectively (Table 2.2). Turn angle concentrations (κ) for resting, transiting, and foraging states were 1.53, 1.48, and 0.81, respectively. Approximately 44% of recorded steps were attributed to resting, 12% to transiting, and 45% to foraging (Table 2.3; Appendix Figures 2A.1 – 2A.5) as determined by the Viterbi algorithm and subsequent calculations.

2.4.2.2 Auklets

Auklet mean step lengths (in meters) for resting, transiting, and foraging were 115 m (SD = 119), 839 m (SD = 1028 m), and 508 m (SD = 489 m), respectively (Table 2.4). Turn angle concentrations (κ) for resting, transiting, and foraging were 1.73, 55.89, and 0.58, respectively. Approximately 32% of recorded steps were attributed to resting, 52% to transiting, and 15% to foraging (Table 2.3; Appendix Figures 2A.6 – 2A.8).

2.5 DISCUSSION

We used HMMs to estimate movement parameters and behavioral states for two sentinel seabird species that exhibit very different foraging and provisioning strategies during the breeding season.

Despite obtaining reasonable parameter estimates for movements in the transiting states, we had difficulty in producing reasonable estimates for movement parameters in the resting and foraging states. Because of this, we would like to emphasize that the following discussion acknowledges the limited conclusions that can be drawn from our estimates. We found average resting step lengths for guillemots and auklets at 94m and 115m, respectively, which was intended to reflect stationary periods while birds were either roosting in nest boxes or burrows or were resting on the water. Regardless of the reasons the birds may have been resting, these estimates far exceeded expected values. One potential reason may be due to the models' inability to distinguish steps associated with resting and foraging given that both states involve shorter step lengths. This possibility is supported by predicted state sequences (Figures 2.4 – 2.13), nearly all of which show foraging occurring at least partially on Protection Island. As seabirds, neither guillemots nor auklets forage on land. One approach to address this issue would involve setting the resting state based on the location of birds, and restricting transitions into the resting state otherwise. This would require developing a rule for setting the resting state, such as when birds are within a certain proximity of the estimated nest location. Given that guillemots are known to sit on the water just offshore from the island with bill loads after foraging trips, but also may forage in the same area, setting this rule would require careful evaluation of its impact on results.

Our models' conflation of resting and foraging states likewise impacted our estimate of time spent resting by guillemots (44%). This high value may be attributed in part to two features of their behavior. First, guillemots are known to roost at nests in their breeding colonies at night (Johns and Warzybok, 2022), which is when most of the gaps in our tracking data occurred. Multiple imputation may have played a role in overestimation of step lengths if, for instance, the uncertainty of imputed points that accounted for periods when birds were resting in nest boxes or burrows caused what would otherwise be stationary points to oscillate around their "true" location". Another factor resulting in the high amount of time spent resting may be the amount of time guillemots spend floating offshore with food before delivering it to their young. We have observed this in individuals at Protection Island, and this behavior

has been reported elsewhere (Bishop et al., 2016; 2018; Molina and Cook, 2022). This floating behavior may be driven by a few different factors. First, guillemots are known to drift with currents and obtain food in a somewhat passive manner, diving occasionally and then resurfacing without moving significantly from their original location (Holm and Burger, 2002). Second, predation risk may influence this behavior. We have observed Bald Eagles (*Haliaeetus leucocephalus*) harassing and attacking the birds along the beaches on Protection Island, and potential territorial competition between guillemots and co-occurring gull species may play a role in influencing this behavior. While resting offshore is common and well documented, it may be that guillemots return to their nests in groups to minimize risk.

Estimates of transiting behavior appeared reasonable, as indicated by figures 2.4 – 2.13. Directed movements that appear to reflect travel between foraging sites or between the island and foraging sites are largely identified as transit. We found the average guillemot transiting step length to be 903 m (Table 2.2), and never observed guillemots traveling more than 10 km from nest sites (Figures 2.4 – 2.8). While we did not attempt to identify foraging habitat, it clearly exists within this range given that guillemots generally did not leave the areas immediately surrounding Protection Island (Figures 2.4 – 2.8). Literature describing frequent daily provisioning (Emms and Verbeek, 1991; Bishop et al., 2016) is supported by our estimates of proportion of time spent in each behavioral state (Table 2.2). Our model indicated that breeding guillemots spent about 45% of their time foraging and only 12% transiting (see Appendix Figures 2A.1 – 2A.5). Our low estimate of time spent transiting, though clearly not fully accurate, suggests relatively rapid trips between nests and foraging sites. Guillemots, which have been observed to renest in the same location over many years at Protection Island (Robinson, Pendleton, and Converse; unpublished data) and elsewhere (Nelson, 1991), return to breeding sites around late February to early March, and may use previous experience to quickly locate productive foraging areas.

Our estimates of auklet movement parameters were somewhat different than those for guillemots, though these also featured inaccurate estimates for resting step lengths, and likely turn angle concentration. We estimated higher step lengths in resting and foraging states (Table 2.3), which were

about 20 m and 500 m greater than guillemot step lengths, respectively. Longer foraging step lengths may make sense given the foraging and provisioning strategies of auklets, which are not as spatially constrained in their foraging movements as guillemots. Similarly, that we can see them traveling much farther distances during daily activities (Figures 2.9 – 2.13) may be why we estimated such a high concentration for transiting step lengths ($\kappa = 55.89$).

Whereas guillemots spent most of their time either resting or foraging, auklets were estimated to spend 32% of their time resting, 52% transiting, and 15% foraging (Table 2.4; see Appendix Figures 2A.6 – 2A.8). Auklets were observed traveling much farther distances to forage (Figures 2.9 – 2.13), passing southeast through Admiralty Inlet and north to the southern end of the San Juan Islands. These distances are similar to previous observations of auklets in the Strait of Juan de Fuca (Wahl and Speich, 1994) and are reflected in the greater estimated proportion of time spent transiting (Table 2.4). Comparing state-dependent step lengths and time spent in each state in years of contrasting marine productivity may yield more information about how both species acclimate to adverse conditions. For instance, lower prey abundance or quality may push birds to travel greater distances to secure reliable food sources, or they may spend more time overall in transiting or foraging states due to increased foraging effort to meet the energetic demands of the breeding season.

The tags we attached to birds failed to collect about 52% of the data that could have been collected across the duration of tag lifespans. Given that these missing data were apparently primarily due to tags being unable to communicate with satellites while birds were in nest boxes or burrows, it is worth noting how these species' time budgets may have resulted in missing such a large amount of data. Guillemots show an inverse correlation between resting time and foraging activity (Litzow and Piatt, 2003), the latter of which is determined by prey abundance and prey specialization by the foraging guillemots. This inverse relationship, with specific values varying based on prey access, is true for auklets as well (Davoren, 2000). While there will always be a portion of missing data due to the inability of tags to communicate with satellites while birds are roosting, future researchers may find it useful to monitor

prey deliveries to chicks as a measure of foraging effort. Though the amount of data loss is at least partially dependent on environmental conditions, and despite existing methods to address spatial or temporal irregularity in records, minimizing collection error and increasing precision is critical to obtaining high quality telemetry data. One way to achieve this is to reduce tag loss due to the attachment method used. We used waterproof, cloth tape to attach tags to monitored birds, which is conventional in seabird tracking (Wilson et al., 1997; Freeman et al., 2010; Harris et al., 2012). This method allowed tags to fall off naturally as birds preened their feathers, molted, or due to other mechanical disturbances. While tags were expected to fall off and were expected to miss data as birds returned to nest boxes or burrows, methods to increase the length of time that birds carry tags could improve future results from tracking studies.

Straightforward and reproducible methods to monitor, describe, and classify seabird movement patterns play a key role in understanding how they operate within their environment. While we had difficulty in producing accurate estimates of state-dependent movement parameters, we describe next steps to address these issues. The outcomes of this research emphasize the importance of having some understanding of a species' behavior prior to attempting to model movements, and in understanding the limitations of using HMMs to infer behavioral states. Additionally, this study highlights the potential benefit of specifying when behavioral states may be explicitly known, such that models are able to accurately estimate these states. By employing GPS tracking and hidden Markov modeling, our study is one of the first to attempt to quantify movement parameters of guillemots and auklets in the Salish Sea. Future work can improve upon our approach to obtain more accurate inferences of these species' underlying behavioral states and can better inform their use as indicators of the marine environment.

2.6 REFERENCES

Beaubier, J., & Hipfner, J. M. (2013). Proximate composition and energy density of forage fish delivered to Rhinoceros Auklet *Cerorhinca* monocerata nestlings at Triangle Island, British Columbia. Marine Ornithology 41, 35-39.

Bell, W. J. (1990). Central place foraging. In W. J. Bell (Ed.), Searching behaviour: The behavioural ecology of finding resources (pp. 171–187). Springer Netherlands. https://doi.org/10.1007/978-94-011-3098-1_12

Beumer, L. T., Pohle, J., Schmidt, N. M., Chimienti, M., Desforges, J.-P., Hansen, L. H., Langrock, R., Pedersen, S. H., Stelvig, M., & van Beest, F. M. (2020). An application of upscaled optimal foraging theory using hidden Markov modelling: Year-round behavioural variation in a large arctic herbivore. Movement Ecology, 8(1), 25. https://doi.org/10.1186/s40462-020-00213-x

Bishop, E., Rosling, G., Kind, P., & Wood, F. (2016). Pigeon Guillemots on Whidbey Island, Washington: a six-year monitoring study. Northwestern Naturalist, 97(3), 237–245. https://doi.org/10.1898/NWN15-31.1

Breed, G. A., Costa, D. P., Jonsen, I. D., Robinson, P. W., & Mills-Flemming, J. (2012). State-space methods for more completely capturing behavioral dynamics from animal tracks. Ecological Modelling, 235–236, 49–58. https://doi.org/10.1016/j.ecolmodel.2012.03.021

Buckner, E., Chittaro, P., Wood, F., & Klinger, T. (2022). Identifying dietary preferences in breeding Pigeon Guillemot (*Cepphus columba*) using different methods. Northwestern Naturalist, 103(1), 42–50. https://doi.org/10.1898/1051-1733-103.1.42

Cairns, D. K., Bredin, K. A., & Montevecchi, W. A. (1987). Activity budgets and foraging ranges of breeding Common Murres. The Auk, 104(2), 218–224. https://doi.org/10.1093/auk/104.2.218

Chimienti, M., Cornulier, T., Owen, E., Bolton, M., Davies, I. M., Travis, J. M. J., & Scott, B. E. (2017). Taking movement data to new depths: Inferring prey availability and patch profitability from seabird foraging behavior. Ecology and Evolution, 7(23), 10252–10265. https://doi.org/10.1002/ece3.3551

Cleasby, I. R., Wakefield, E. D., Morrissey, B. J., Bodey, T. W., Votier, S. C., Bearhop, S., & Hamer, K. C. (2019). Using time-series similarity measures to compare animal movement trajectories in ecology. Behavioral Ecology and Sociobiology, 73(11), 151. https://doi.org/10.1007/s00265-019-2761-1

Critchley, E. J., Grecian, W. J., Bennison, A., Kane, A., Wischnewski, S., Cañadas, A., Tierney, D., Quinn, J. L., & Jessopp, M. J. (2020). Assessing the effectiveness of foraging radius models for seabird distributions using biotelemetry and survey data. Ecography, 43(2), 184–196. https://doi.org/10.1111/ecog.04653

Davoren, G. K. (2000). Variability in foraging in response to changing prey distributions in Rhinoceros Auklets. Marine Ecology Progress Series. 198, 283–291.

Elliott, K. H., Woo, K., Gaston, A. J., Benvenuti, S., Dall'Antonia, L., & Davoren, G. K. (2008). Seabird foraging behaviour indicates prey type. Marine Ecology Progress Series, 354, 289–303. https://doi.org/10.3354/meps07221

Evans, K., Lea, M.-A., & Patterson, T. A. (2013). Recent advances in bio-logging science: Technologies and methods for understanding animal behaviour and physiology and their environments. Deep

Sea Research Part II: Topical Studies in Oceanography, 88–89, 1–6. https://doi.org/10.1016/j.dsr2.2012.10.005

Freeman, R., Dennis, T., Landers, T., Thompson, D., Bell, E., Walker, M., & Guilford, T. (2010). Black Petrels (*Procellaria parkinsoni*) patrol the ocean shelf-break: GPS tracking of a vulnerable Procellariiform seabird. PLOS ONE, 5(2), e9236. https://doi.org/10.1371/journal.pone.0009236

Fromant, A., Delord, K., Bost, C.-A., Eizenberg, Y. H., Botha, J. A., Cherel, Y., Bustamante, P., Gardner, B. R., Brault-Favrou, M., Lec'hvien, A., & Arnould, J. P. Y. (2021). Impact of extreme environmental conditions: foraging behaviour and trophic ecology responses of a diving seabird, the common diving petrel. Progress in Oceanography, 198, 102676. https://doi.org/10.1016/j.pocean.2021.102676

Frey, S., Fisher, J. T., Burton, A. C., & Volpe, J. P. (2017). Investigating animal activity patterns and temporal niche partitioning using camera-trap data: challenges and opportunities. Remote Sensing in Ecology and Conservation, 3(3), 123–132. https://doi.org/10.1002/rse2.60

Gaston, A. J., Ydenberg, R. C., & Smith, G. E. J. (2007). Ashmole's Halo and population regulation in seabirds. Marine Ornithology 34: 119-126.

Godley, B., Blumenthal, J., Broderick, A., Coyne, M., Godfrey, M., Hawkes, L., & Witt, M. (2008). Satellite tracking of sea turtles: where have we been and where do we go next? Endangered Species Research, 4, 3–22. https://doi.org/10.3354/esr00060

Golet, G. H., Kuletz, K. J., Roby, D. D., & Irons, D. B. (2000). Adult prey choice affects chick growth and reproductive success in Pigeon Guillemots. The Auk, 117(1), 82–91. https://doi.org/10.1093/auk/117.1.82

Grémillet, D., Dell'Omo, G., Ryan, P., Peters, G., Ropert-Coudert, Y., & Weeks, S. (2004). Offshore diplomacy or how seabirds mitigate intra-specific competition: a case study based on GPS tracking of Cape Gannets from neighbouring colonies. Marine Ecology Progress Series, 268, 265–279. https://doi.org/10.3354/meps268265

Harris, M. P., Bogdanova, M. I., Daunt, F., & Wanless, S. (2012). Using GPS technology to assess feeding areas of Atlantic Puffins *Fratercula arctica*. Ringing & Migration, 27(1), 43–49. https://doi.org/10.1080/03078698.2012.691247

Holm, K. J., & Burger, A. E. (2002). Foraging behavior and resource partitioning by diving birds during winter in areas of strong tidal currents. Waterbirds, 24(3), 312-325.

Jodice, P. G., & Collopy, M. W. (1999). Diving and foraging patterns of Marbled Murrelets (*Brachyramphus marmoratus*): testing predictions from optimal-breathing models. Canadian Journal of Zoology, 77(9), 1409–1418. https://doi.org/10.1139/z99-113

Johns, M., & Warzybok, P. (2022). Northward migration, molting locations, and winter residency of California breeding Pigeon Guillemots *Cepphus columba*. Marine Ecology Progress Series, 701, 133–143. https://doi.org/10.3354/meps14194

Keating, K. A., Brewster, W. G., & Key, C. H. (1991). Satellite telemetry: performance of animal-tracking systems. The Journal of Wildlife Management, 55(1), 160–171. https://doi.org/10.2307/3809254

Kuletz, K. J. (1998). Pigeon Guillemot *Cepphus columba*. Restoration Notebook.

Lamb, J. S., Loring, P. H., & Paton, P. W. C. (2023). Distributing transmitters to maximize population-level representativeness in automated radio telemetry studies of animal movement. Movement Ecology, 11(1), 1. https://doi.org/10.1186/s40462-022-00363-0

Lee, J. E., White, G. C., Garrott, R. A., Bartmann, R. M., & Alldredge, A. W. (1985). Accessing accuracy of a radiotelemetry system for estimating animal locations. The Journal of Wildlife Management, 49(3), 658–663. https://doi.org/10.2307/3801690

Litzow, M. A., Piatt, J. F., Abookire, A. A., Speckman, S. G., Arimitsu, M. L., & Figurski, J. D. (2004). Spatiotemporal predictability of schooling and nonschooling prey of Pigeon Guillemots. The Condor, 106(2), 410–415. https://doi.org/10.1093/condor/106.2.410

Litzow, M. A., & Piatt, J. F. (2003). Variance in prey abundance influences time budgets of breeding seabirds: evidence from pigeon guillemots *Cepphus columba*. Journal of Avian Biology, 34(1), 54–64. https://doi.org/10.1034/j.1600-048X.2003.02995.x

McClintock, B. T. (2017). Incorporating telemetry error into hidden Markov models of animal movement using multiple imputation. Journal of Agricultural, Biological and Environmental Statistics. https://link.springer.com/article/10.1007/s13253-017-0285-6

McClintock, B. T., & Michelot, T. (2018). momentuHMM: R package for generalized hidden Markov models of animal movement. Methods in Ecology and Evolution, 9(6), 1518–1530. https://doi.org/10.1111/2041-210X.12995 Mech, L. D. (1967). Telemetry as a technique in the study of predation. The Journal of Wildlife Management, 31(3), 492–496. https://doi.org/10.2307/3798129

Michelot, T., & Langrock, R. (2023). A short guide to choosing initial parameter values for the estimation in moveHMM. 1-9.

Miller, M. R., Takekawa, J. Y., Fleskes, J. P., Orthmeyer, D. L., Casazza, M. L., & Perry, W. M. (2005). Spring migration of Northern Pintails from California's Central Valley wintering area tracked with satellite telemetry: toutes, timing, and destinations. Canadian Journal of Zoology, 83(10), 1314–1332. https://doi.org/10.1139/z05-125

Molina, C. and Cook, A. 2022. Pigeon Guillemot Nesting Behavior on San Juan Island, Washington. University of Washington Conservation of Marine Birds and Mammals. 725.

Nakagawa, S., & Freckleton, R. P. (2008). Missing inaction: the dangers of ignoring missing data. Trends in Ecology & Evolution, 23(11), 592–596. https://doi.org/10.1016/j.tree.2008.06.014

Nelson, D. A. (1991). Demography of the Pigeon Guillemot on Southeast Farallon Island, California. The Condor, 93(3), 765–768. https://doi.org/10.2307/1368213

Orians, G. H., & Pearson, N. E. (1979). On the theory of central place foraging. Analysis of Ecological Systems. Ohio State University Press, Columbus, 2, 155-177.

Patel, S. H., Morreale, S. J., Panagopoulou, A., Bailey, H., Robinson, N. J., Paladino, F. V., Margaritoulis, D., & Spotila, J. R. (2015). Changepoint analysis: a new approach for revealing animal movements and behaviors from satellite telemetry data. Ecosphere, 6(12), 1–13. https://doi.org/10.1890/ES15-00358.1

Pattison, V., Bone, C., Cowen, L. L. E., O'Hara, P. D., & Wilson, L. (2023). Characterizing Ancient Murrelet *Synthliboramphus antiquus* movement behaviour during breeding-season foraging trips using hidden Markov models. Ibis, 165(3), 924–943. https://doi.org/10.1111/ibi.13173

Pearson, S.F. & Hamel, N.J. (2013). Marine and terrestrial bird indicators for Puget Sound. Washington Department of Fish and Wildlife and Puget Sound Partnership, Olympia, WA. 55 pp.

Pearson, S. F., Hodum, P. J., Good, T. P., Schrimpf, M., & Knapp, S. M. (2013). A model approach for estimating colony size, trends, and habitat associations of burrow-nesting seabirds. The Condor, 115(2), 356–365. https://doi.org/10.1525/cond.2013.110207

Ropert-Coudert, Y., Grémillet, D., Kato, A., Ryan, P. G., Naito, Y., & Le Maho, Y. (2004). A fine-scale time budget of Cape Gannets provides insights into the foraging strategies of coastal seabirds. Animal Behaviour, 67(5), 985–992. https://doi.org/10.1016/j.anbehav.2003.09.010

Royle, J. A., Chandler, R. B., Sun, C. C., & Fuller, A. K. (2013). Integrating resource selection information with spatial capture–recapture. Methods in Ecology and Evolution, 4(6), 520–530. https://doi.org/10.1111/2041-210X.12039

Saldanha, S., Cox, S. L., Militão, T., & González-Solís, J. (2023). Animal behaviour on the move: the use of auxiliary information and semi-supervision to improve behavioural inferences from hidden Markov models applied to GPS tracking datasets. Movement Ecology, 11(1), 41. https://doi.org/10.1186/s40462-023-00401-5

Stoneburner, D. L. (1982). Satellite telemetry of loggerhead sea turtle movement in the Georgia Bight. Copeia, 1982(2), 400–408. https://doi.org/10.2307/1444621

Sun, A., Whelan, S., Hatch, S. A., & Elliott, K. H. (2020). Tags below three percent of body mass increase nest abandonment by rhinoceros auklets, but handling impacts decline as breeding progresses. Marine Ecology Progress Series, 643, 173–181. https://doi.org/10.3354/meps13341

Tudorache, C., Burgerhout, E., Brittijn, S., & Thillart, G. van den. (2014). The effect of drag and attachment site of external tags on swimming eels: experimental quantification and evaluation tool. PLOS ONE, 9(11), e112280. https://doi.org/10.1371/journal.pone.0112280

Van Der Hoop, J. M., Fahlman, A., Hurst, T., Rocho-Levine, J., Shorter, K. A., Petrov, V., & Moore, M. J. (2014). Bottlenose dolphins modify behavior to reduce metabolic effect of tag attachment. Journal of Experimental Biology, 217(23), 4229–4236. https://doi.org/10.1242/jeb.108225

Vermeer, K., & Devito, K. (1986). Size, caloric content, and association of prey fishes in meals of nestling Rhinoceros Auklets. The Murrelet, 67(1), 1–9. https://doi.org/10.2307/3535529

Wagner, E. L., Pearson, S. F., Good, T. P., Hodum, P. J., Buhle, E. R., & Schrimpf, M. B. (2023). Resilience to a severe marine heatwave at two Pacific seabird colonies. Marine Ecology Progress Series, HEAT. https://doi.org/10.3354/meps14222

Wahl, T. R., & Speich, S. M. (1994). Distribution of foraging Rhinoceros Auklets in the Strait of Juan de Fuca, Washington. Northwestern Naturalist, 75(2), 63–69. https://doi.org/10.2307/3536766

Watanuki, Y., Yamamoto, M., Okado, J., Ito, M., & Sydeman, W. (2022). Seabird reproductive responses to changing climate and prey communities are mediated by prey packaging. Marine Ecology Progress Series, 683, 179–194. https://doi.org/10.3354/meps13943

Weimerskirch, H., & Wilson, R. P. (2000). Oceanic respite for wandering albatrosses. Nature, 406(6799), 955–956. https://doi.org/10.1038/35023068

Wilson, R. P., Pütz, K., Peters, G., Culik, B., Scolaro, J. A., Charrassin, J.-B., & Ropert-Coudert, Y. (1997). Long-term attachment of transmitting and recording devices to penguins and other seabirds. Wildlife Society Bulletin (1973-2006), 25(1), 101–106.

Wilson, U. W., & Manuwal, D. A. (1986). Breeding biology of the Rhinoceros Auklet in Washington. The Condor, 88(2), 143–155. https://doi.org/10.2307/1368909

Wilson, U. W. (1977). A study of the biology of the Rhinoceros Auklet on Protection Island, Washington. Doctoral dissertation, University of Washington.

Zhang, J., Rayner, M., Vickers, S., Landers, T., Sagar, R., Stewart, J., & Dunphy, B. (2019). GPS telemetry for small seabirds: using hidden Markov models to infer foraging behaviour of Common Diving Petrels (*Pelecanoides urinatrix urinatrix*). Emu - Austral Ornithology, 119(2), 126–137. https://doi.org/10.1080/01584197.2018.1558997

Zucchini, W., MacDonald, I.L. & Langrock, R. (2016). Hidden Markov Models for Time Series: An Introduction Using R, 2nd edn. Boca Raton: CRC Press.

2.7 FIGURES AND TABLES

Table 2.1 Summary of Pigeon Guillemot (PIGU) and Rhinoceros Auklet (RHAU) tagging data recorded by GPS tags in 2022 and 2023 at Protection Island, Washington, USA. Featured tags are those that were able to be processed and used in analysis (except see footnote). Tag ID, date range of data collected, number of collected points, and number of missing points are shown. Location coordinates were collected every 15 minutes. Missing points are calculated by the number of points missed in between observations where time elapsed is greater than 15 minutes.

Species	Tag ID	Date Range	Collected Points	Missing Points	% Missed
PIGU	44067	23/06/2022 – 02/07/2022	731	831	53
	44072	22/06/2022 – 29/06/2022	499	672	57
	44372[a]	29/06/2022 – 30/06/2022	160	93	37
	44505	22/06/2022 – 05/07/2022	1066	1202	53
	45657	13/07/2023 – 21/07/2023	627	115	16
	45658	13/07/2023 – 16/07/2023	181	266	60
RHAU	44149	23/06/2022 – 23/06/2022	32	28	47
	45653[a]	13/07/2023 – 13/07/2023	30	31	51
	45659[a]	13/07/2023 – 14/07/2023	88	105	54
	45663	13/07/2023 – 22/07/2023	620	858	58
	45672	13/07/2023 – 21/07/2023	638	780	55
	45695	13/07/2023 –14/07/2023	65	174	73
	45701	13/07/2023 – 13/07/2023	49	58	54

[a]Data from these tags were not able to be imputed using the crawlWrap function from the momentuHMM package (version 2.0.0; McClintock and Michelot, 2018). These tracks were omitted from analysis.

Table 2.2 Summary of hidden Markov model (HMM) outputs for movement parameters of behavioral state classifications of breeding Pigeon Guillemots tracked in 2022 and 2023 at Protection Island, Washington, USA. Mean step length and standard deviation (meters) and turn angle concentration (unitless) are shown for each state.

State	Step Length (meters; θ, σ)	Turn Angle (κ)
Resting	93 ± 87	1.53
Transiting	903 ± 1022	1.47
Foraging	13 ± 16	0.81

Table 2.3 Percentage of time spent in each behavioral state (resting, transiting, and foraging) of tracked, breeding Pigeon Guillemots (PIGU) and Rhinoceros Auklets (RHAU) at Protection Island, Washington, USA in 2022 and 2023 as estimated by hidden Markov models (HMMs). Percentages were derived from state sequences as computed by the Viterbi algorithm.

Species	Time Resting (%)	Time Transiting (%)	Time Foraging (%)
PIGU	44	12	45
RHAU	32	52	15

Table 2.4 Summary of hidden Markov model (HMM) outputs for movement parameters of behavioral state classifications of breeding Rhinoceros Auklet tracked in 2022 and 2023 at Protection Island, Washington, USA. Mean step length and standard deviation (meters) and turn angle concentration (unitless) are shown for each state.

State	Step Length (meters; θ, σ)	Turn Angle (κ)
Resting	115 ± 119	1.73
Transiting	839 ± 1028	55.89
Foraging	508 ± 489	0.58

Figure 2.1 Protection Island, Jefferson County, Washington, which includes the US Fish and Wildlife Service's Protection National Wildlife Refuge and the Washington Department of Fish and Wildlife's Zella M. Schultz Seabird Sanctuary. The Seabird Sanctuary is comprised of Kanem Point (on the southwest end of the island) and the area just to the north of Kanem Point.

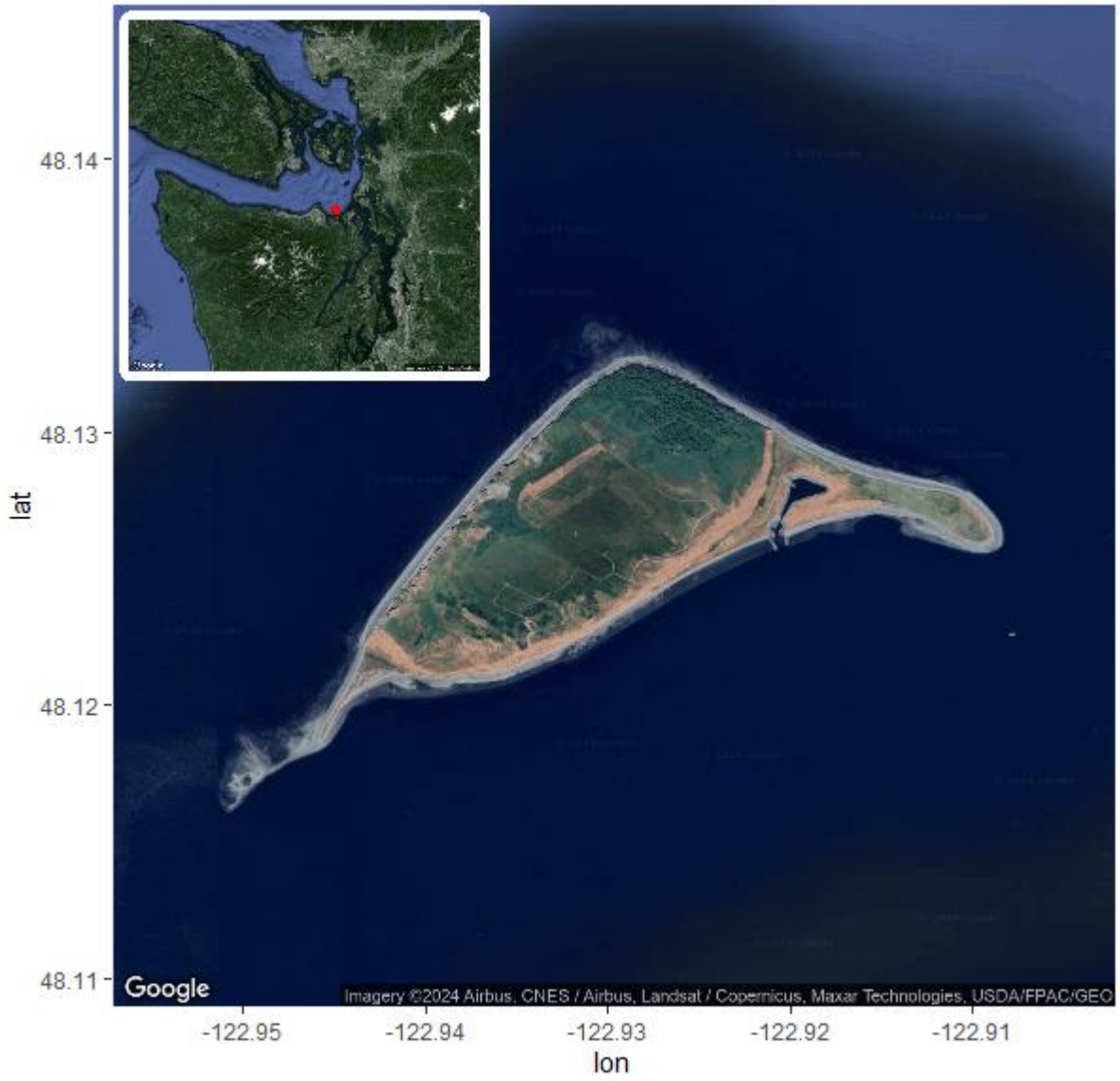

Figure 2.2 Locations of nests of tracked birds and base stations used in analysis from 2022 on Protection Island, Washington, USA. Yellow diamonds indicate nests where Pigeon Guillemots were tagged, and the green diamond indicates the bluff where Rhinoceros Auklets were tagged. Because auklets were captured randomly on the bluff marked by the green diamond and were not tracked to their burrow, one marker is used. The large blue diamond indicates the location of the base station used to receive GPS data.

Figure 2.3 Locations of nests of tracked birds and base stations used in analysis from 2023 on Protection Island, Washington, USA. Yellow diamonds indicate nests where Pigeon Guillemots were tagged, and the green diamond indicates the bluff where Rhinoceros Auklets were tagged. Because auklets were captured randomly on the bluff marked by the green diamond and were not tracked to their burrow, one marker is used. The large blue diamonds indicate the locations of the base stations used to receive GPS data.

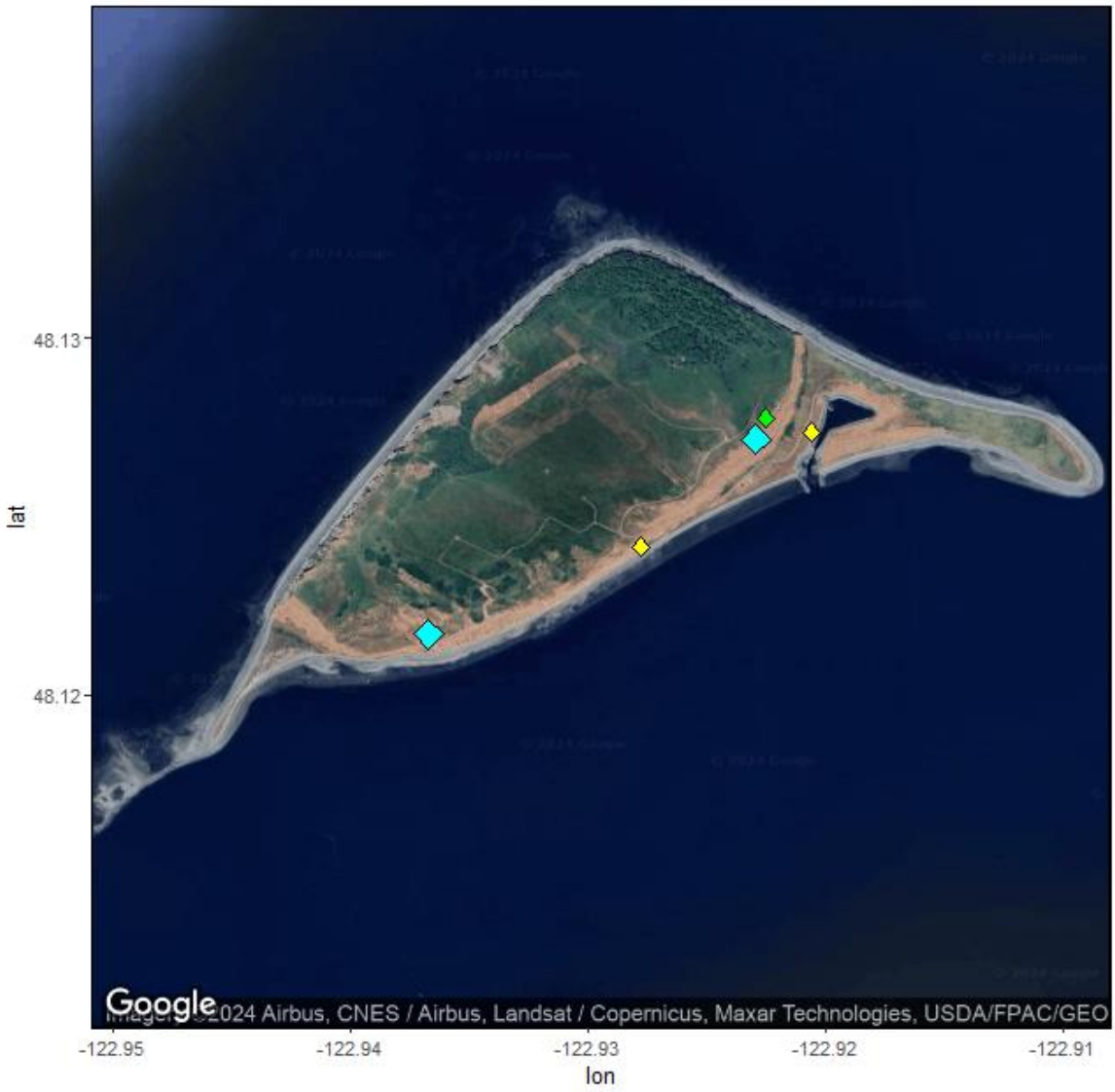

Figure 2.4 Plot of track from Pigeon Guillemot #44067 at Protection Island, Washington, USA (left), plot of the Viterbi-decoded state sequence for the 3-state hidden Markov model (resting, transiting, and foraging) model (right). Track plot is measured in latitude/longitude, and Viterbi plot is measured in UTMs.

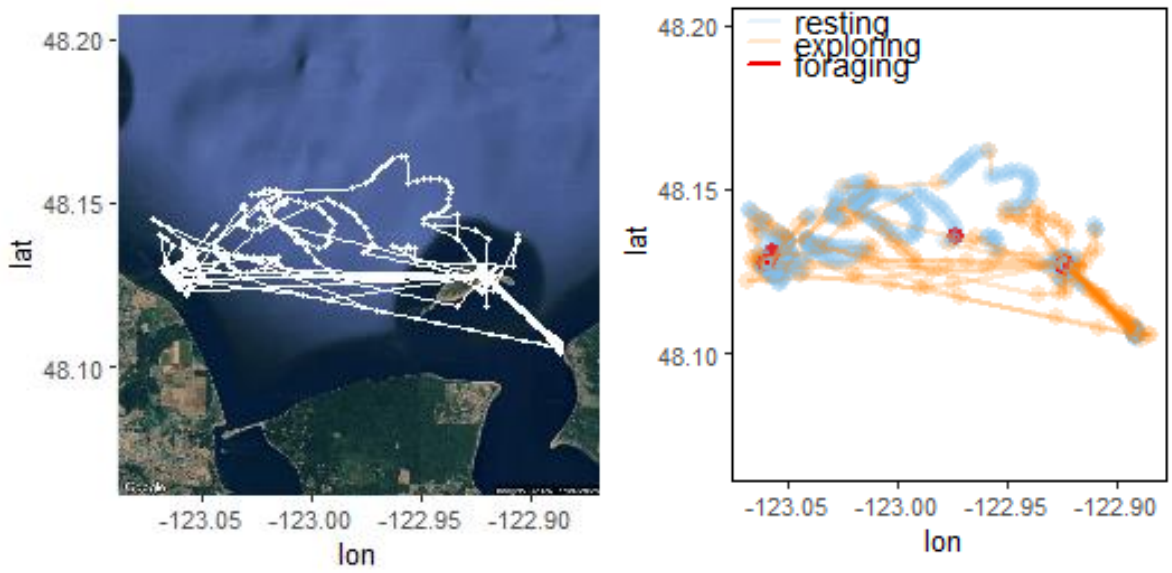

Figure 2.5 Plot of track from Pigeon Guillemot #44072 at Protection Island, Washington, USA (left), plot of the Viterbi-decoded state sequence for the 3-state hidden Markov model (resting, transiting, and foraging) model (right). Track plot is measured in latitude/longitude, and Viterbi plot is measured in UTMs.

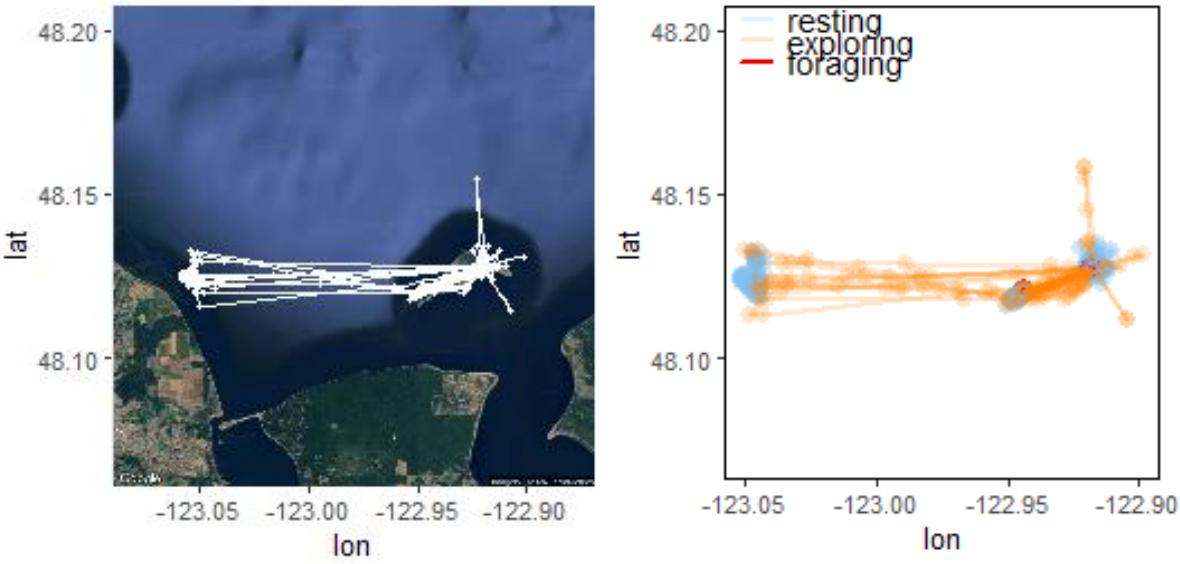

Figure 2.6 Plot of track from Pigeon Guillemot #44505 at Protection Island, Washington, USA (top-left), plot of the Viterbi-decoded state sequence for the 3-state hidden Markov model (resting, transiting, and foraging) model (right). Track plot is measured in latitude/longitude, and Viterbi plot is measured in UTMs.

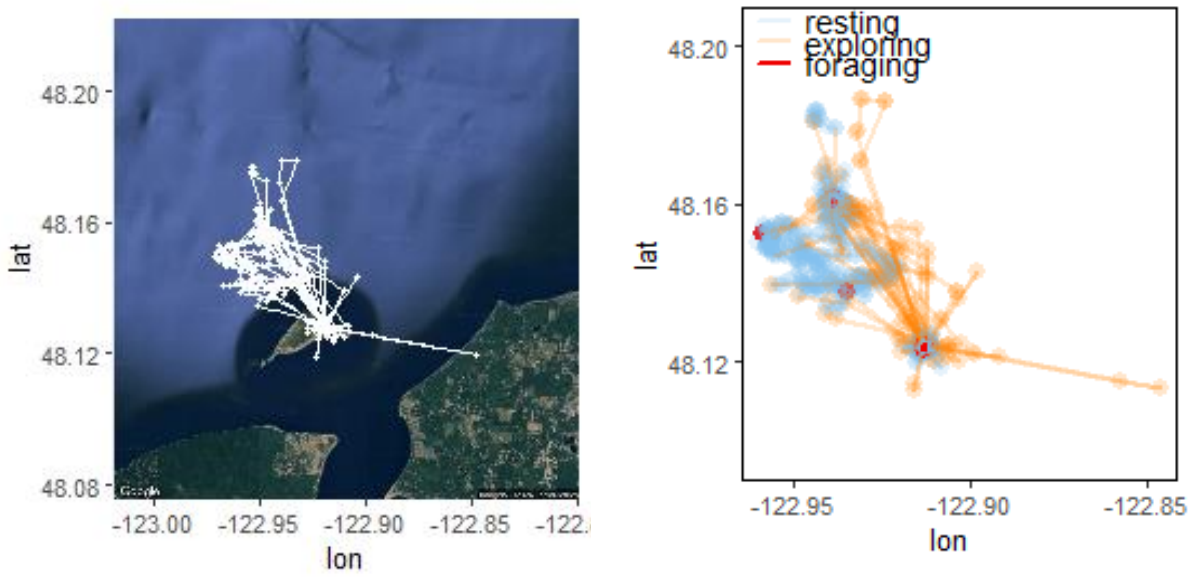

Figure 2.7 Plot of track from Pigeon Guillemot #45657 at Protection Island, Washington, USA (top-left), plot of the Viterbi-decoded state sequence for the 3-state hidden Markov model (resting, transiting, and foraging) model (right). Track plot is measured in latitude/longitude, and Viterbi plot is measured in UTMs.

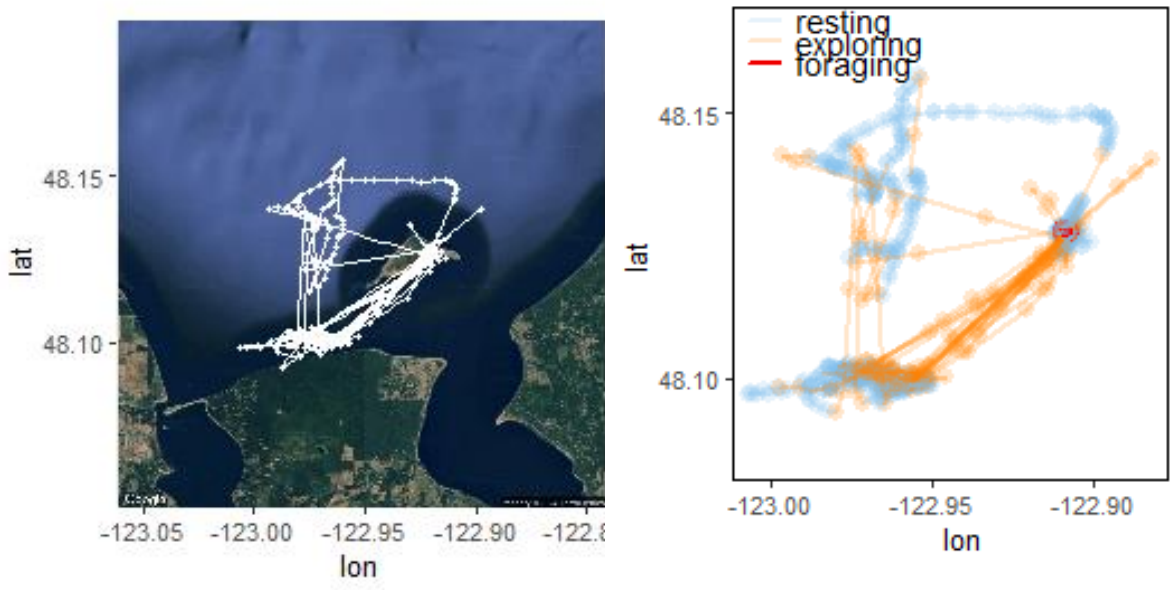

Figure 2.8 Plot of track from Pigeon Guillemot #45658 at Protection Island, Washington, USA (top-left), plot of the Viterbi-decoded state sequence for the 3-state hidden Markov model (resting, transiting, and foraging) model (right). Track plot is measured in latitude/longitude, and Viterbi plot is measured in UTMs.

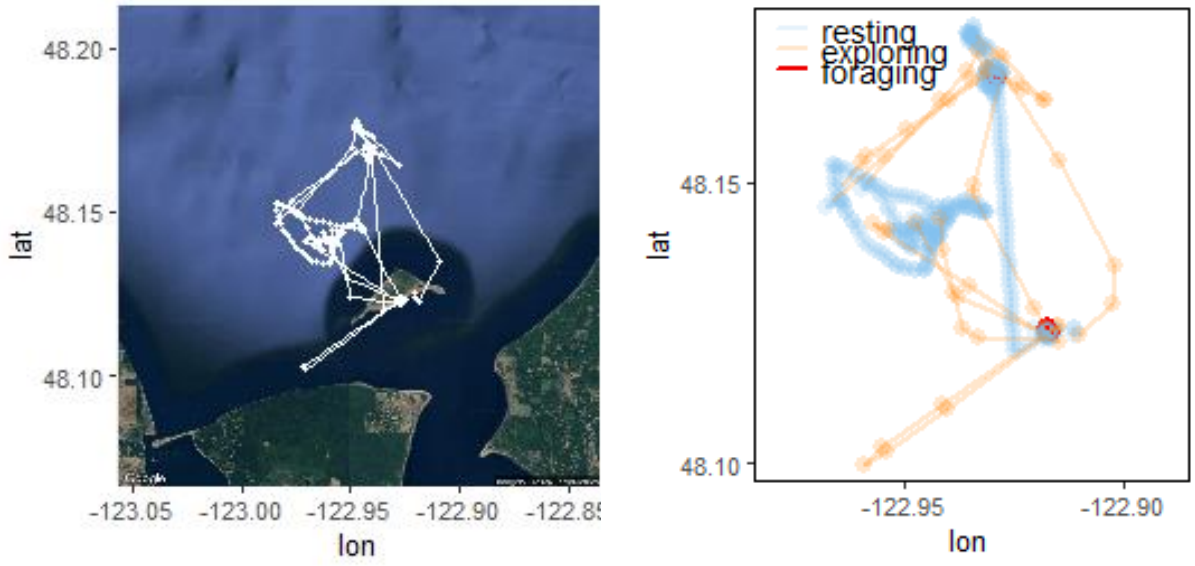

Figure 2.9 Plot of track from Rhinoceros Auklet #44149 at Protection Island, Washington, USA (top-left), plot of the Viterbi-decoded state sequence for the 3-state hidden Markov model (resting, transiting, and foraging) model (right). Track plot is measured in latitude/longitude, and Viterbi plot is measured in UTMs.

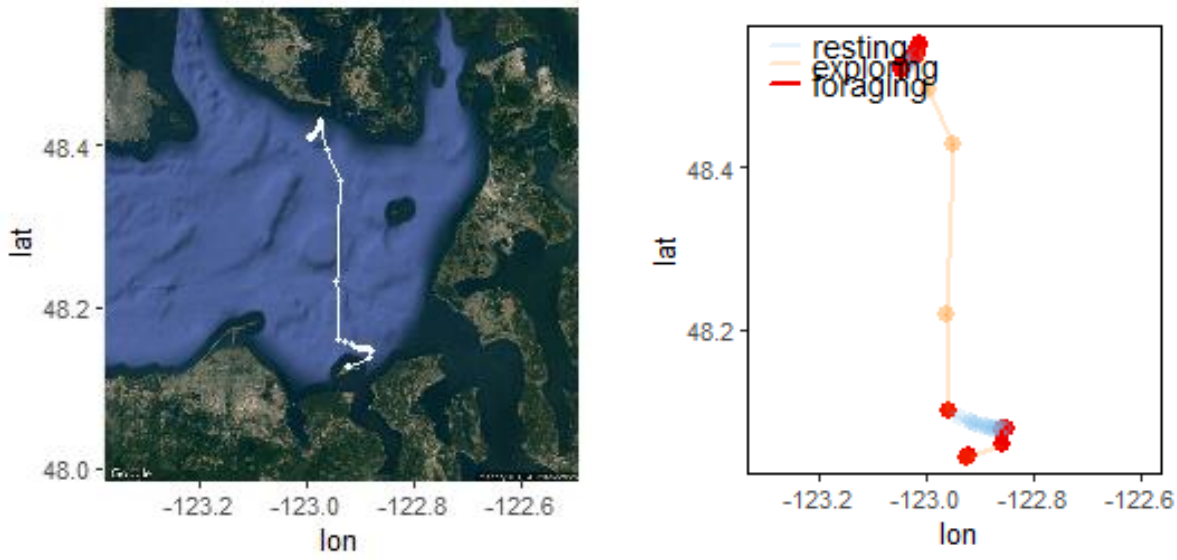

Figure 2.10 Plot of track from Rhinoceros Auklet #45663 at Protection Island, Washington, USA (top-left), plot of the Viterbi-decoded state sequence for the 3-state hidden Markov (resting, transiting, and foraging) model (right). Track plot is measured in latitude/longitude, and Viterbi plot is measured in UTMs.

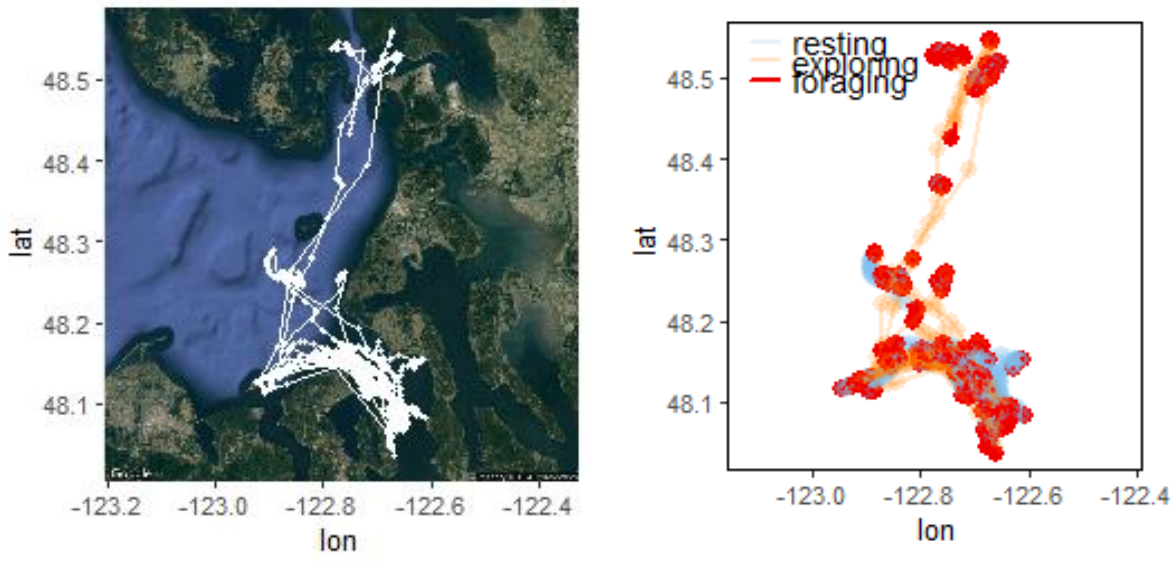

Figure 2.11 Plot of track from Rhinoceros Auklet #45672 at Protection Island, Washington, USA (top-left), plot of the Viterbi-decoded state sequence for the 3-state hidden Markov model (resting, transiting, and foraging) model (right). Track plot is measured in latitude/longitude, and Viterbi plot is measured in UTMs.

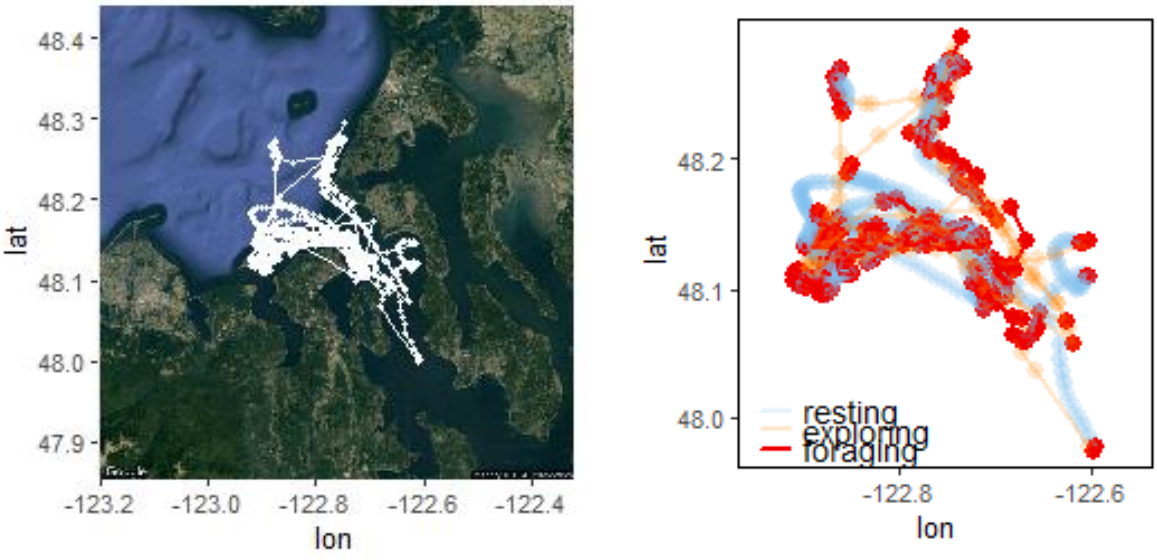

Figure 2.12 Plot of track from Rhinoceros Auklet #45695 at Protection Island, Washington, USA (top-left), plot of the Viterbi-decoded state sequence for the 3-state hidden Markov model (resting, transiting, and foraging) model (right). Track plot is measured in latitude/longitude, and Viterbi plot is measured in UTMs.

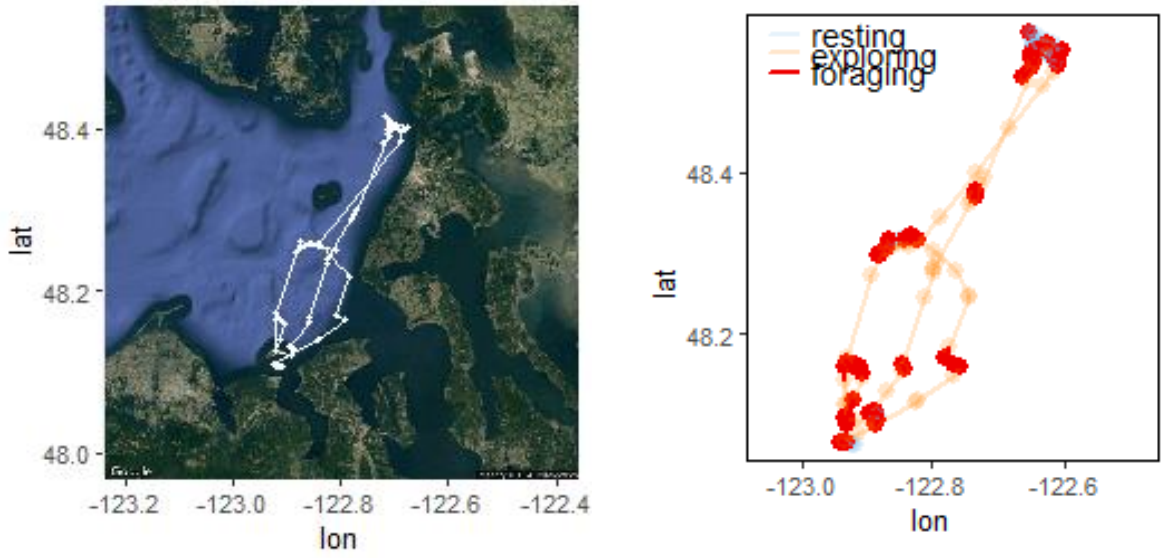

Figure 2.13 Plot of track from Rhinoceros Auklet #45701 at Protection Island, Washington, USA (top-left), plot of the Viterbi-decoded state sequence for the 3-state hidden Markov model (resting, transiting, and foraging) model (right). Track plot is measured in latitude/longitude, and Viterbi plot is measured in UTMs.

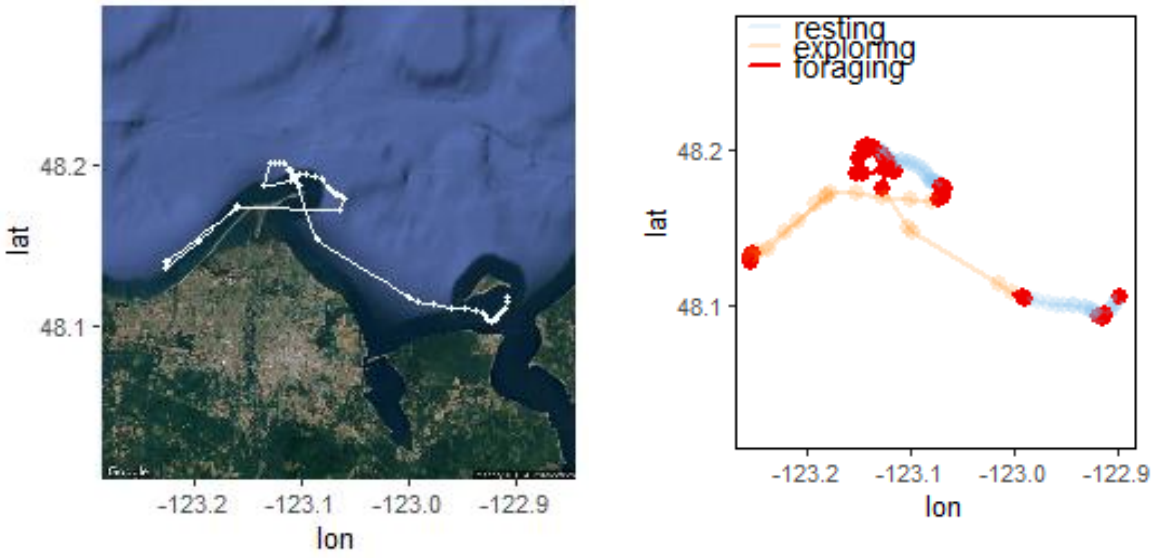

2.8 APPENDIX A

Figure 2A.1 Plots of step length (meters; on the log scale), turn angle, and state sequence for Pigeon Guillemot #44067 descending respectively.

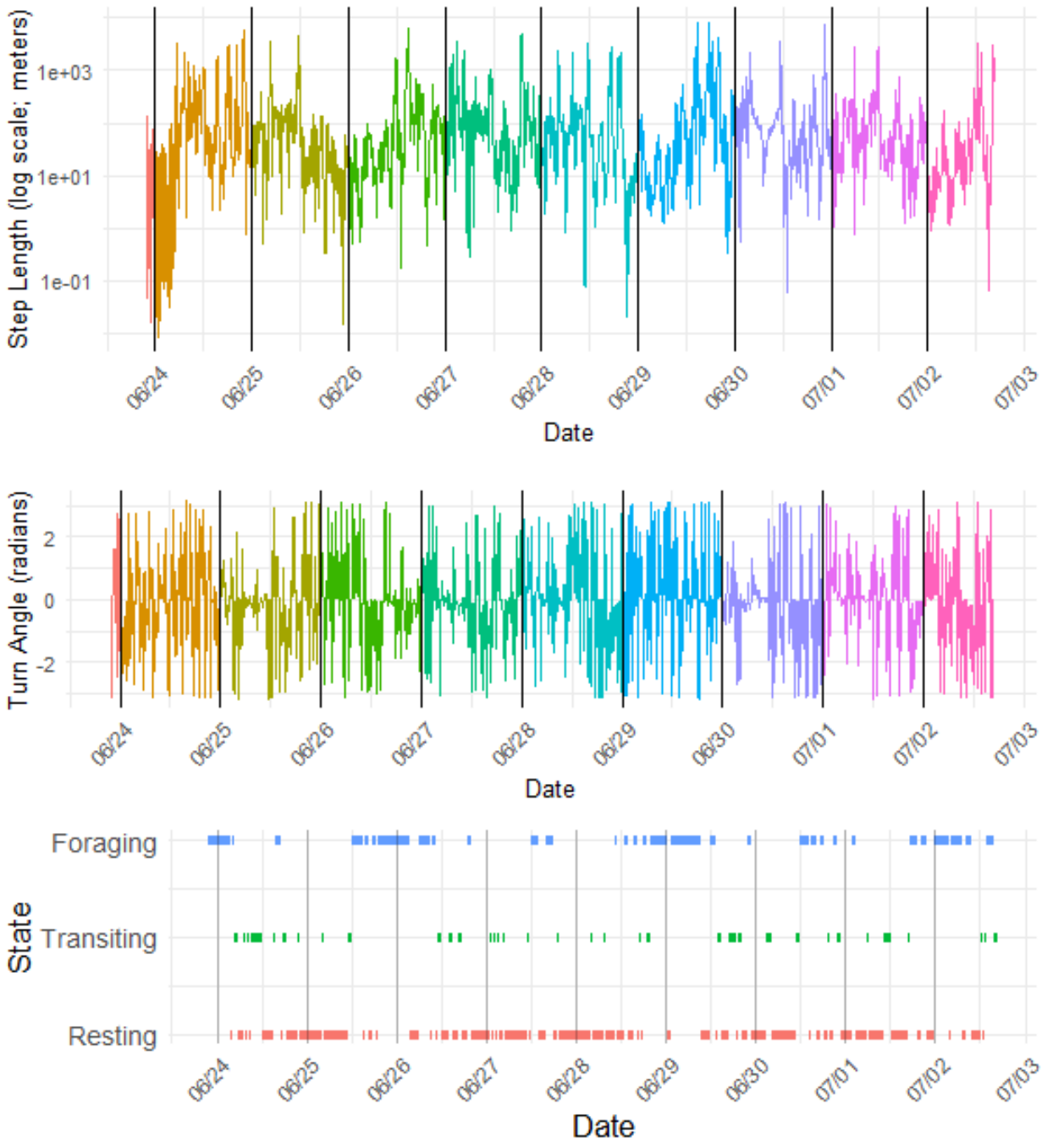

Figure 2A.2 Plots of step length (meters; on the log scale), turn angle, and state sequence for Pigeon Guillemot #44072 descending respectively.

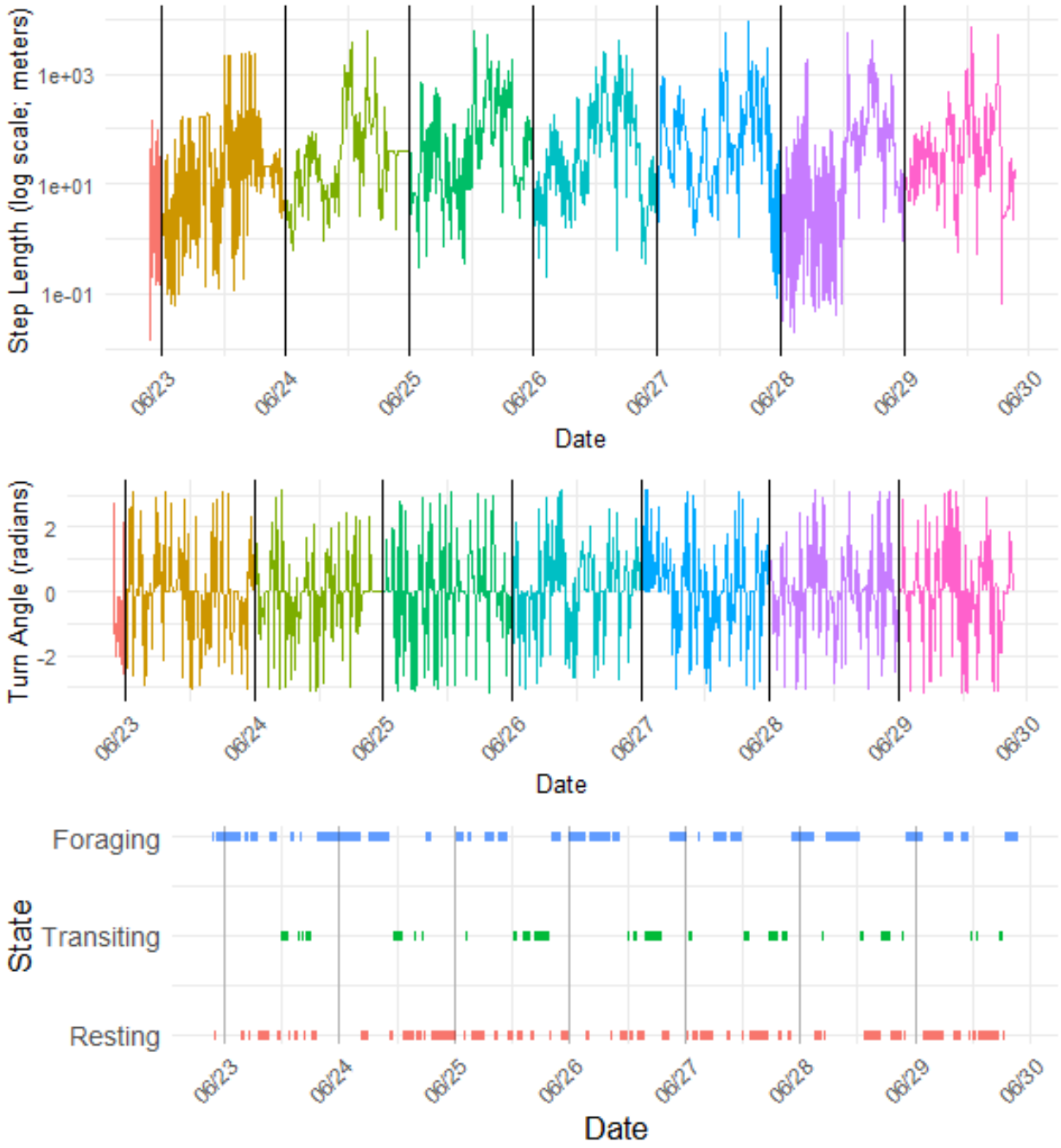

Figure 2A.3 Plots of step length (meters; on the log scale), turn angle, and state sequence for Pigeon Guillemot #44505 descending respectively.

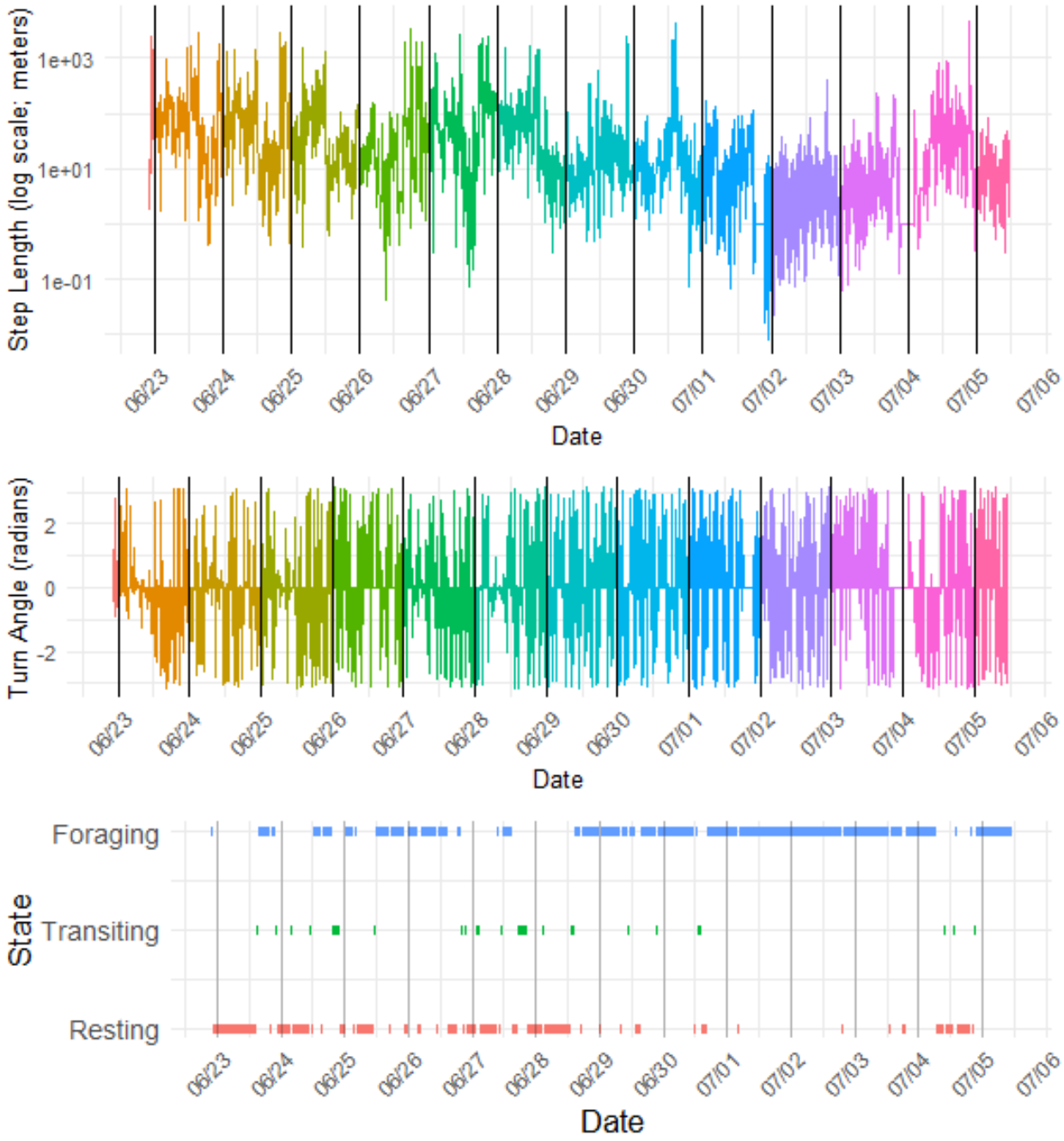

Figure 2A.4 Plots of step length (meters; on the log scale), turn angle, and state sequence for Pigeon Guillemot #45657 descending respectively.

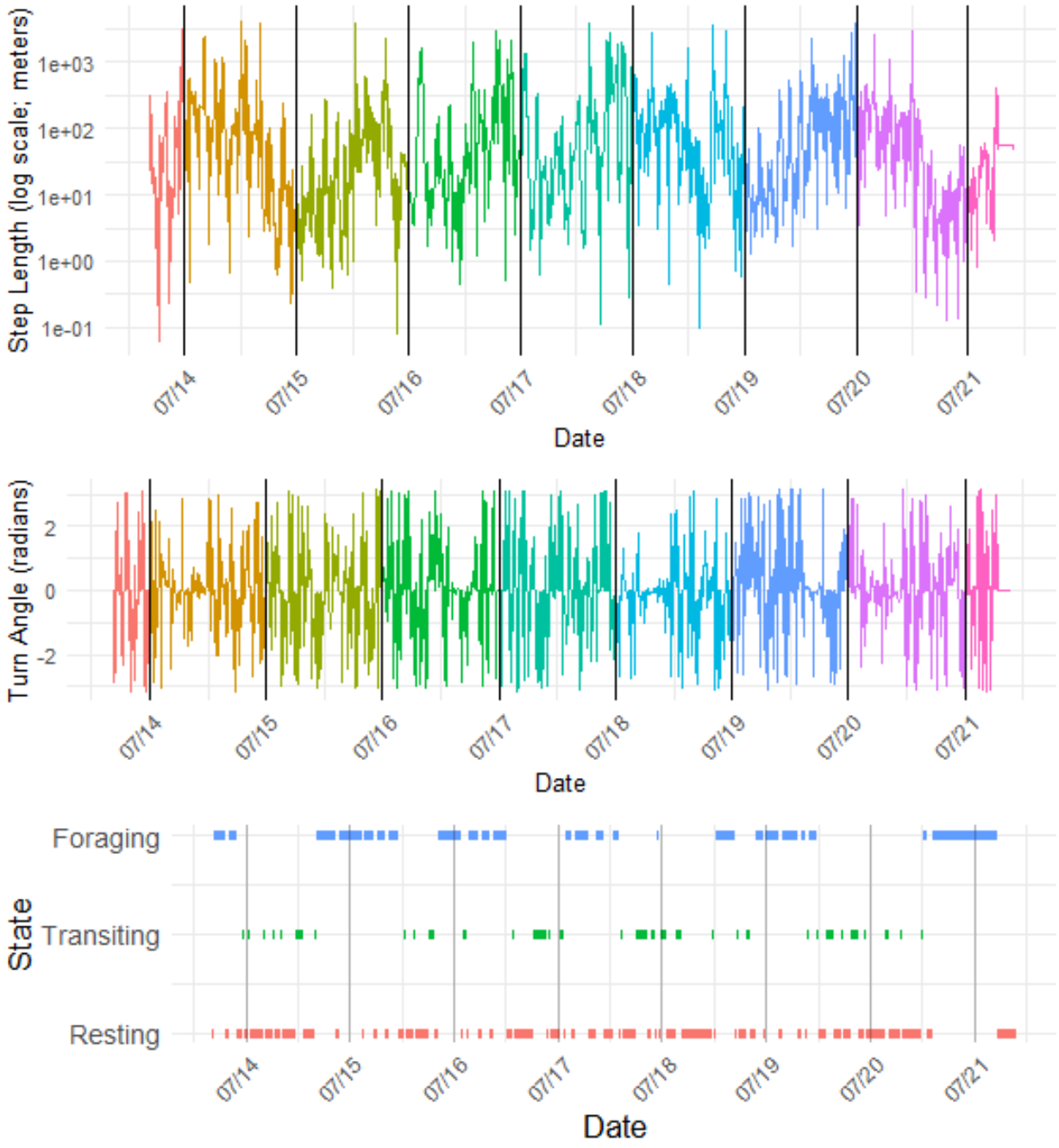

Figure 2A.5 Plots of step length (meters; on the log scale), turn angle, and state sequence for Pigeon Guillemot #45658 descending respectively.

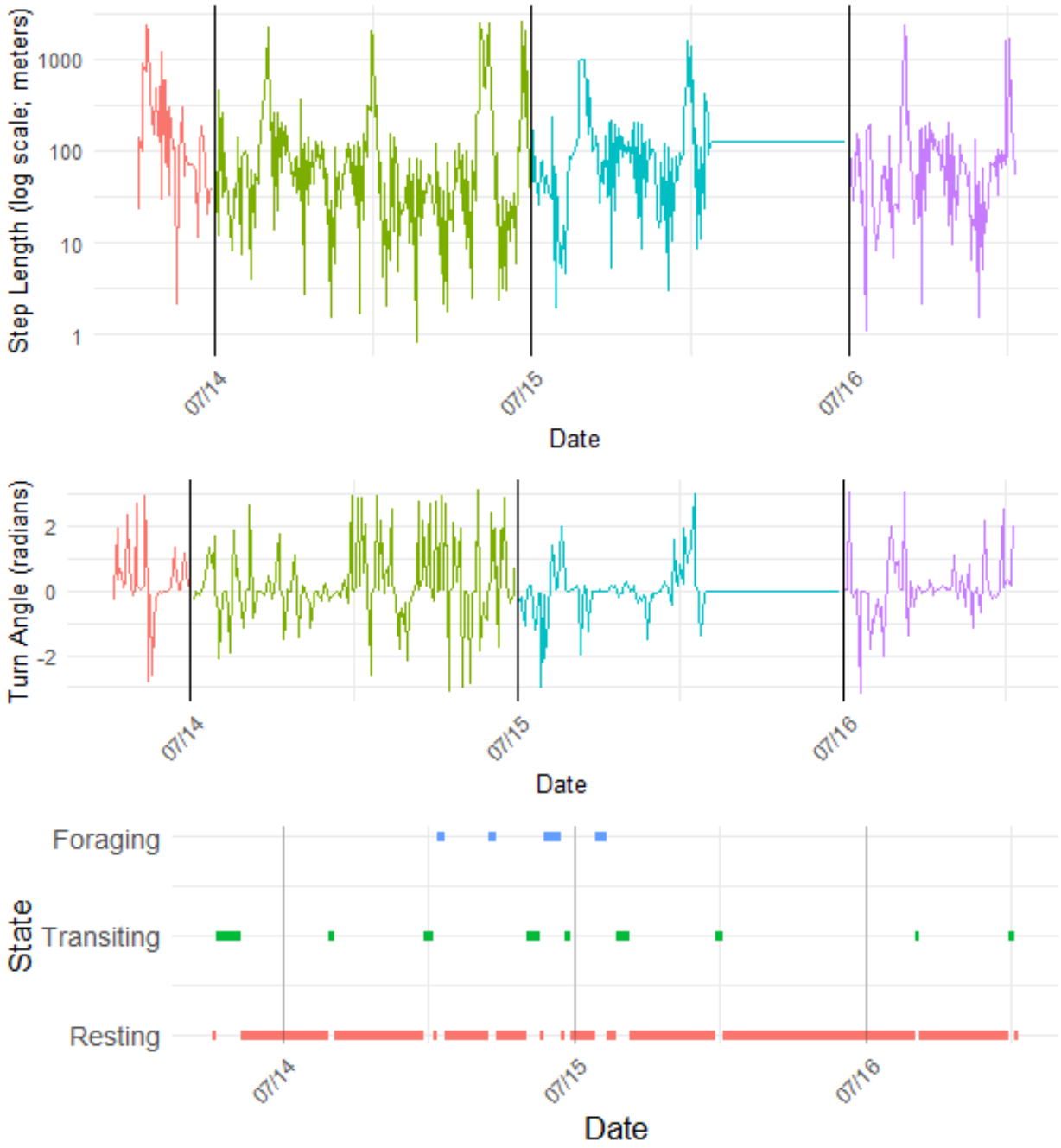

Figure 2A.6 Plots of step length (meters; on the log scale), turn angle, and state sequence for Rhinoceros Auklet #45663 descending respectively.

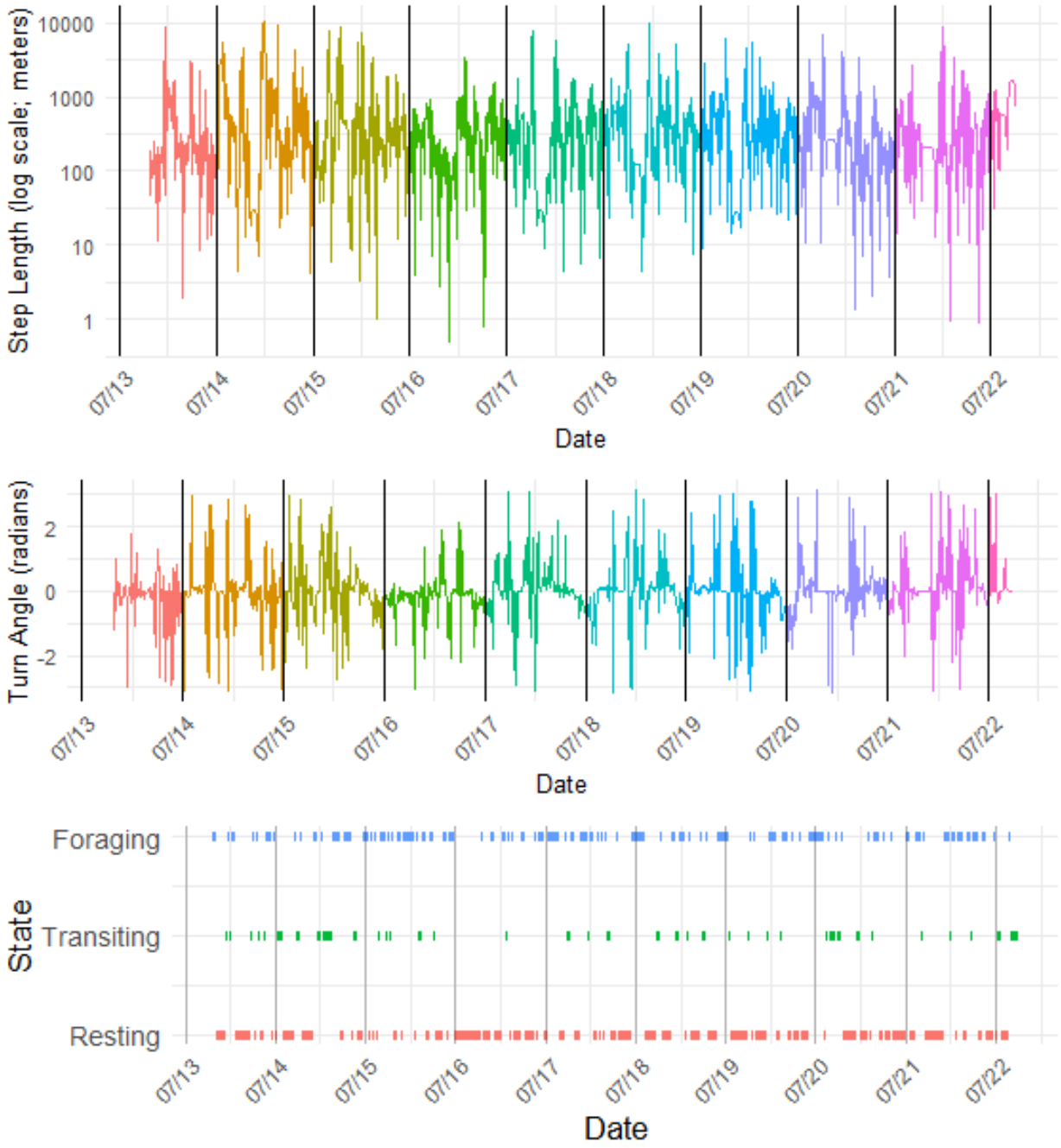

Figure 2A.7 Plots of step length (meters; on the log scale), turn angle, and state sequence for Rhinoceros Auklet #45672 descending respectively.

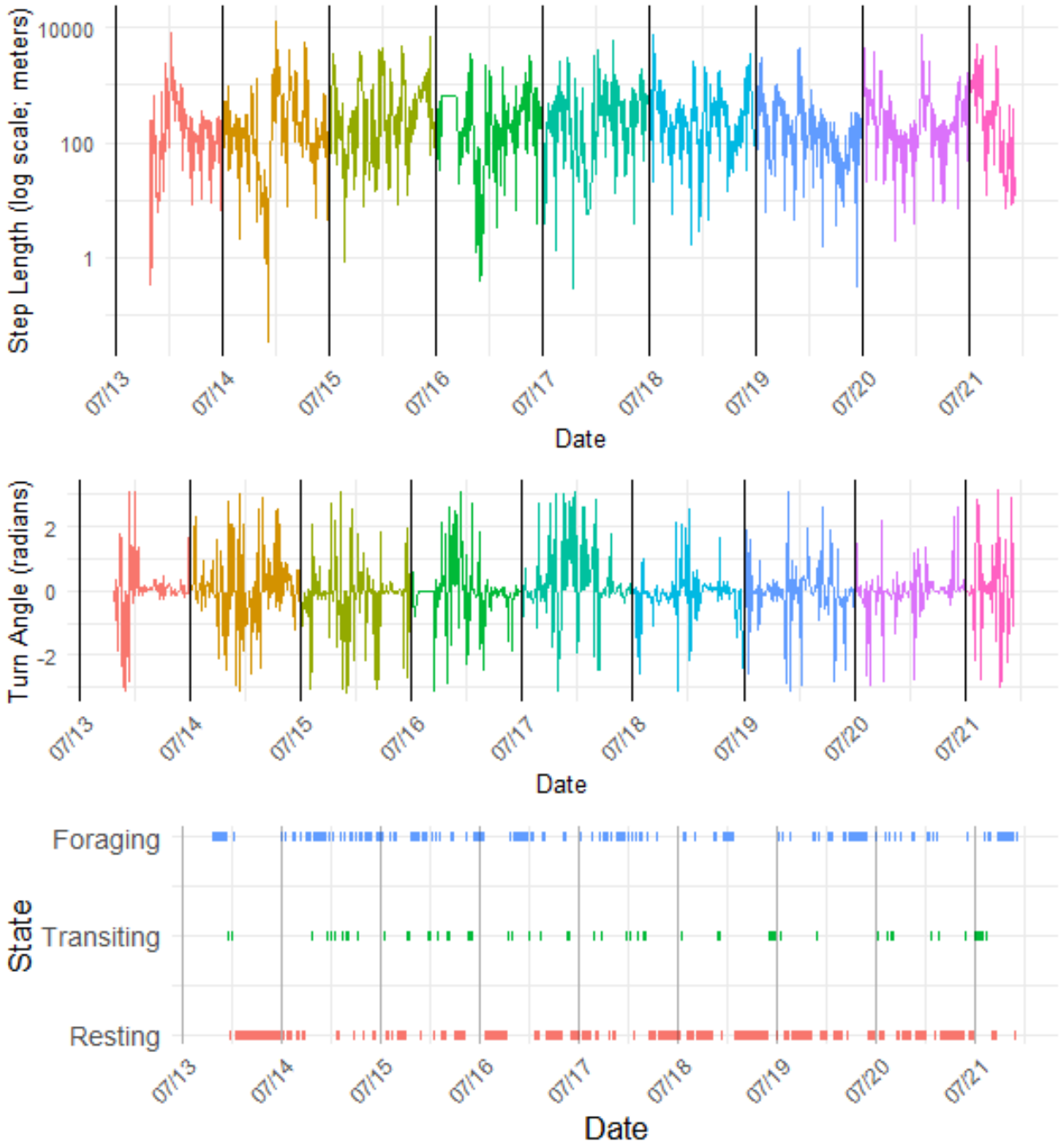

Figure 2A.8 Plots of step length (meters; on the log scale), turn angle, and state sequence for Rhinoceros Auklet #45695 descending respectively.